INVESTIGATIONS ON NANOFILLER INCORPORATED PEMA COMPOSITE ELECTROLYTES FOR LITHIUM BATTERIES

(File No.42-819/2013(SR), dated 22.3.2013)

Final Progress Report
for the period 1.4.2013 to 31.3.2017

Submitted to

UNIVERSITY GRANTS COMMISSION
BAHADUR SHAH ZAFAR MARG
NEW DELHI – 110 002

By
Dr. M.RAMESH PRABHU
Assistant Professor
Principal Investigator- UGC-MRP
FUEL CELL AND ENERGY RESEARCH LAB, Department of Physics
Science Block, Alagappa University
Karaikudi-630 003, Tamil Nadu

Annexure – IX

UNIVERSITY GRANTS COMMISSION
BAHADUR SHAH ZAFAR MARG
NEW DELHI – 110 002

PROFORMA FOR SUBMISSION OF INFORMATION AT THE TIME OF SENDING THE FINAL REPORT OF THE WORK DONE ON THE PROJECT

1. Title of the Project: '**INVESTIGATIONS ON NANOFILLER INCORPORATED PEMA COMPOSITE ELECTROLYTES FOR LITHIUM BATTERIES**

2. NAME AND ADDRESS OF THE: **Dr. M.RAMESH PRABHU**,
PRINCIPAL INVESTIGATOR: **Assistant Professor,**
Department of Physics,
Alagappa University,
Karaikudi – 630 003.

3. NAME AND ADDRESS OF THE INSTITUTION: **Alagappa University,**
Karaikudi – 630 003.

4. UGC APPROVAL LETTER NO. AND DATE: **File No.42-819/2013(SR), dated 22.3.2013.**
DATE OF IMPLEMENTATION: 01.04.2013

6. TENURE OF THE PROJECT: **01.04.2013 to 31.3.2017**

7. TOTAL GRANT ALLOCATED: **Rs.9,36,542/-**

8. TOTAL GRANT RECEIVED: **Rs.8,71,168/-**

9. FINAL EXPENDITURE: **Rs.8,71,168/-**

10. TITLE OF THE PROJECT: **'INVESTIGATIONS ON NANOFILLER INCORPORATED PEMA COMPOSITE ELECTROLYTES FOR LITHIUM BATTERIES'**

i. OBJECTIVES OF THE PROJECT

Origin of the research problem

For future energy generation and conservation, a rapid growth in research and development relating to "polymer electrolytes" is a necessity. The impetus for studying the fundamental aspects of polymer – salt systems has come about largely through the desire to develop thin –film rechargeable lithium batteries based on these materials. Michel Armand proposed the use of polymer –like materials for the fabrication of thin–flim, rechargeable lithium batteries, and this idea has gained increasing popularity and attention. Over the last decade several academic, government and industrial laboratories have been engaged in the development of this fascinating battery concept.

Polymer electrolytes have occupied an important position in solid state ionics, because of their unique properties. Namely they have thin film forming property, good processability, flexibility, light weight, elasticity and transparency as well as relatively high ionic conductivity and wide potential window in the solid states. Some of these characteristics cannot be attained by hard inorganic solid electrolytes, including glasses and thus have been exploited to bridge a gap between fluid electrolyte solutions and hard inorganic solid electrolytes.

Interdisciplinary relevance

Field of Solid State Ionics involving polymer electrolytes is an interdisciplinary subject which needs the knowledge of Physics, Chemistry and Material Science. For the preparation of polymer electrolyte one must have a thorough knowledge of materials science and for further characterization such as XRD, FTIR and SEM etc. needs a wider knowledge of physical chemistry. A thorough knowledge of charge/discharge and cycling of the battery is required for the fabrication of battery. Hence the proposed project work is of interdisciplinary in nature.

Objectives

- To synthesize PEMA – MX – Y – Z [MX = $LiClO_4$, $LiAsF_6$, $LiBF_4$; Y = Plasticizer – EC, PC, DEC and Z = CNT, TiO_2, $BaTiO_3$, etc.] type solvent free composite polymer blend electrolyte.

- To characterize these composite polymeric electrolytes by ac/dc ionic conductivity measurement, complex impedance analysis, electronic conductivity measurement, ionic transport number determination, XRD, FTIR, DSC, SEM, etc.
- A successful polymer membrane will be tested as electrolyte in $Li/LiMn_2O_4$ electrochemical cell couple.

Methodology

Synthesis of PEMA based composite polymer blend electrolytes:

The polymer electrolytes will be prepared by dissolving poly (ethyl methacrylate) and lithium salt in (THF, DMF etc.,) along with suitable plasticizers (PC, EC, DEC, DMP, DEP etc) and ceramics like (CNT, TiO_2, $BaTiO_3$, etc.,) followed by casting onto a teflon sheet.

Preparation of polymer films for conductivity measurements:

Appropriate amounts of PEMA and ($LiClO_4$, $LiBF_4$, $LiAsF_6$ etc) will be dissolved along with suitable plasticizers along with ceramics. The film will be dried in a vacuum oven at 40^0 C with a pressure of 10^{-1} torr. The dried thin film will be sandwiched between polished stainless steel electrodes and finally loaded in a sample holder for conductivity studies.

i. WORK DONE SO FAR

A. Preparation of polymer electrolyte films

Poly (vinyl chloride) (PVC) (Aldrich) and poly (ethyl methacrylate) (PEMA) (Aldrich) and $LiClO_4$ (Aldrich) were dried under vacuum at 100° C for 10 h. The polymer electrolytes of various blend ratios were first dissolved in THF separately and mixed together. The mixture was stirred continuously for about 24 hours. The obtained homogeneous viscous slurry was degassed to remove air bubbles and was poured to the petri dish. The solvent was allowed to evaporate slowly from the complex at 60°C for 6 hours. The solution thus obtained was cast on a glass plate and THF was allowed to evaporate slowly in air at room temperature for 48 hours. This procedure provides mechanically stable, free standing and flexible films with thickness between 1and 2 mm. The films are further dried for 5 hours in vacuum at 60°C to remove any trace of THF. The polymer blends of (PVC: PEMA) blend ratio with constant salt concentration are prepared with different double plasticizers concentration.

Structural Analysis

The X-ray diffraction analysis is a useful tool to determine the structure and crystallization of the polymer matrices in order to investigate the effect of double plasticizer concentrations in the PVC-PEMA-$LiClO_4$ system. XRD analysis has been performed, and their respective diffraction patterns of PVC, PEMA, $LiClO_4$ and their complexes with different double plasticizer concentrations are shown in fig 1.1.

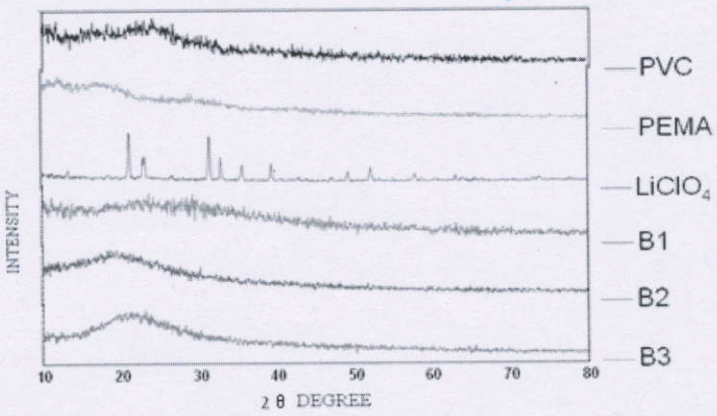

Fig. 1.1. XRD patterns of pure prepared electrolyte membranes

The XRD pattern of $LiClO_4$ shows intense peaks at an angle 2θ =18.36°, 23.2°, 27.5°, 32.99° and 36.58°, which reveals crystalline nature of the ionic salt (JCPDS:030-0751). Fig.1.1 shows one broad peak at an angle 2θ=13°, which corresponds to PVC and shows diffraction peak at 2θ=18°, which is ascribed to PEMA. The diffractograms of PVC-PEMA blend with double plasticizer clearly indicate the fact that the semi crystalline nature of PVC structure is disturbed by the addition of plasticizers and salt. The increase in the amorphous nature causes a reduction in the energy barrier to the segmental motion of the polymer electrolyte. The XRD pattern shows that most of the peaks corresponding to pure $LiClO_4$ disappear in the blend polymer electrolytes, which reveals the complete resolution of the salts in the polymer matrix.

Conductivity Studies

The ionic conductivity of PVC/PEMA based gel polymer electrolytes containing double plasticizers (EC/PC) were calculated from $\sigma = t/R_bA$, where 't' and 'A' represents the thickness and area of the film respectively. R_b is the bulk resistance of the gel electrolyte obtained from complex impedance measurement.

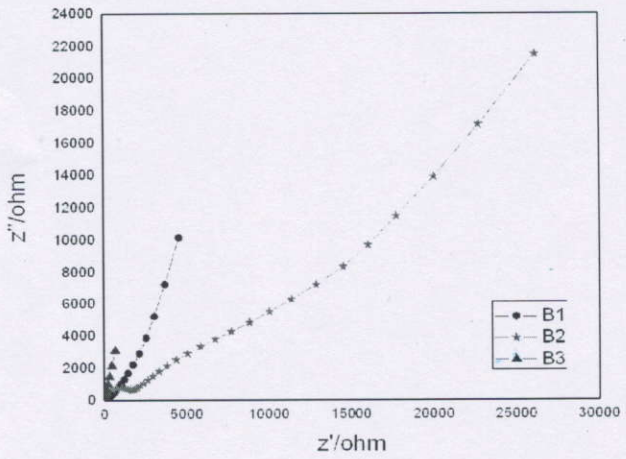

Fig. 1.2. Room temperature complex impedance plot of the prepared samples

Fig. 1.2 shows the room temperature complex impedance spectra of PVC (5) - PEMA (20) - $LiClO_4$ (8) wt % - PC/EC (67%) polymer electrolyte system. According to the theoretical analysis given by Watanabe and Ogata two semicircles should appears in impedance spectrum for a symmetric cell, i.e., one at higher frequencies corresponding to bulk electrolyte impedance and other at lower frequencies related to the interfacial impedance. Also it is reported that the high frequency semicircle does not appear in practical impedance plots for plasticized polymer

electrolyte membranes. The disappearance of semicircle portion indicates that the conductivity is mainly due to ions.

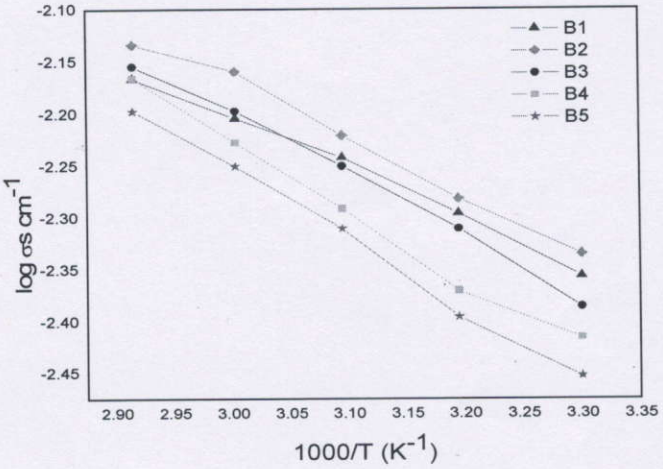

Fig.1.3. Temperature dependent ionic conductivity plots of the prepared samples

Figure.1.3 shows the conductivity versus temperature inverse plots of PVC-PEMA-EC/PC-$LiClO_4$ based hybrid polymer electrolytes. The figure shows that the ionic conduction in all polymer electrolyte systems obeys the VTF (Vogel-Tammam-Fulcher) relation, which describes the transport properties in a viscous matrix . It supports the idea that the ions move through the plasticizer rich phase, which is the conductivity medium and involves the salt.

Table 1.1

Ionic conductivity values of PVC (5) / PEMA (20) / EC+PC (x) / $LiClO_4$ (8) wt. % of the total polymer weight.

Sample coding	**PVC(5)PEMA(20)EC /PC (x) - $LiClO_4$(8) Wt.%**	**Ionic conductivity values (σ)×10^{-3} Scm^{-1} at different temperatures (K)**				
		303	**313**	**323**	**333**	**343**
B1	100/0	4.403	5.061	5.732	6.246	6.812
B2	75/25	4.626	5.231	6.013	6.926	7.346
B3	50/50	4.113	4.892	5.623	6.346	7.003
B4	25/75	3.842	4.261	5.116	5.923	6.826
B5	0/100	3.524	4.021	4.892	5.621	6.346

The conductivity data for hybrid polymer electrolytes containing double plasticizers are presented in table 1.1. From the table we can see that the $LiClO_4$ offers highest conductivity (4.626 x 10^{-3} S cm^{-1}) among the other gel electrolytes at 303K.

Thermal Analysis

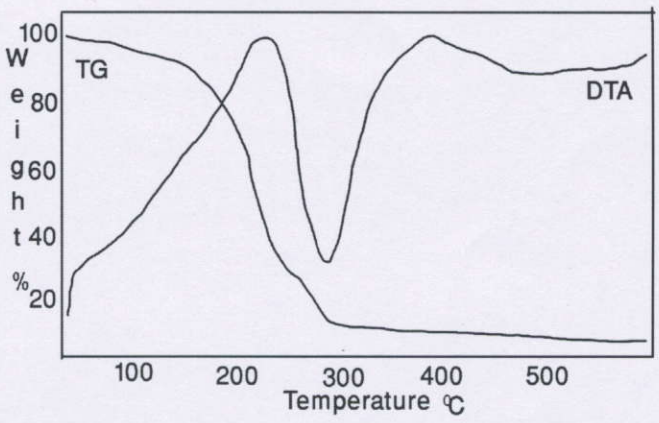

Fig.1.4. TG/DTA analysis of PVC (5)-PEMA (20)-EC/PC (67)-$LiClO_4$ (8)wt%

Figure.1.4 shows the TG/DTA traces of PVC (5)-PEMA (20)-EC/PC (67)-$LiClO_4$ (8) gel polymer electrolyte which shows maximum conductivity value. An endothermic peak was observed at 65°C and corresponding about 5% of weight loss is attributed to the presence of moisture in the samples. The film starts decomposing at 230°C followed by an endothermic peak, which indicates that the film is stable up to 230°C. The DTA trace shows an endothermic peak around 288°C, which corresponds to the melting point of PEMA polymer host.

It is clear from these observations, that the PEMA based hybrid polymer electrolytes, which contain $LiClO_4$ as salt can be operated up to 230°C.

Conclusion

PEMA based blend polymer electrolytes are prepared by solvent casting technique. The complex formation in PEMA-PVC-$LiClO_4$-EC-PC has been confirmed from XRD studies. Ionic and thermal conductivity of the polymer electrolytes were studied. The ionic conductivity of the systems at different temperatures was plotted by using the Arrhenius plot. Good thermal stability of the blend polymer electrolyte system up to 4.626×10^{-3} has been confirmed by TG/DTA analysis.

The ionic conductivity increases with increase in temperature and the highest ionic conductivity has been found to be 4.626×10^{-3} S cm^{-1} at room temperature. This could be used as an electrolyte in lithium batteries and other electrochemical devices.

B. **Preparation of polymer electrolyte films**

All the samples were prepared by facile solution casting technique. The host polymer PEMA, the filler TiO_2 the lithium salts (Sigma Aldrich, USA) heated to 100 °C to remove moisture. The plasticizer Propylene Carbonate (PC) was used as received. The appropriate amounts of the selected polymer and Lithium salts were dissolved using a solvent, tetrahydrofuran (THF) with the help of continuous magnetic stirring to obtain a homogeneous mixture. The plasticizer was added with mixture & the stirring was continued for approximately 24 hours. The obtained slurry was degassed to remove air bubbles and then poured on a well cleaned Teflon covered glass plate to allow the solvent to evaporate at room temperature. The electrolyte films were heated at 60 °C for 6 hours to remove any trace of the residual solvent. X-ray diffraction patterns of the samples were obtained using a computer controlled X'pert propanalytical diffractometer with cu-Kα radiation (wavelength = 0.1541 nm) as the source at 40KV with a scanning range of 10-80°. The AC impedance electrical conductivity study was carried out on the polymer electrolyte film with stainless steel blocking electrodes using a computer controlled Micro-Autolab TYPE III potentiostat/galvanostat in the frequency range of 40 Hz-300 KHz for various temperatures ranging from 302 K to 363 K. TG-DTA thermal analysis of polymer electrolyte samples was performed using a Perkin Elmer pyris-6 TG/DTA with the scan rate of 10 °C min^{-1}.

Structural Analysis

XRD patterns of pure PEMA, $LiClO_4$, TiO_2 and their complexes are shown in the Fig. 2.1. In order to investigate the complexation of lithium salt with the polymer, XRD studies were performed. The amorphous nature of the PEMA and crystalline nature of $LiClO_4$ salt are observed. The characteristic peaks at 18.6° for PEMA reveals the increasing nature in salt concentration. The intensity of PEMA peak decreases and leads, peak appears as single broad peak in the complexes.

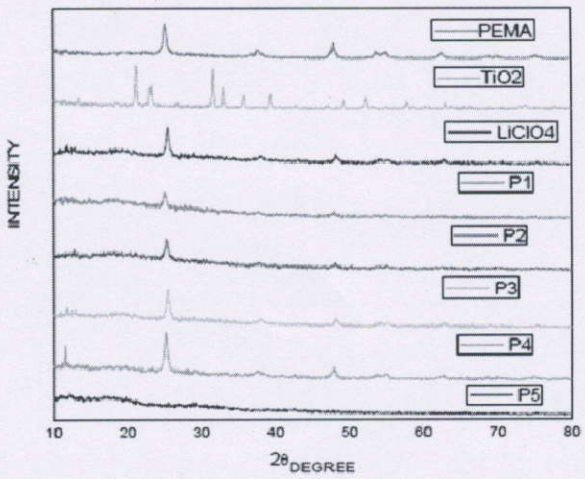

Fig. 2.1. XRD Patterns of pure PEMA, $LiClO_4$, TiO_2 and prepared electrolyte membranes.

The crystallinity of the electrolytes is greatly reduced by the addition of salt and plasticiser. The addition of PC induces significant disorder in the polymer structure, resulting in lower crystallinity. The nanosized TiO_2 emulsion can penetrate the space between the polymer chains and consequently the homogenously dispersed ceramic filler in the matrix prevents and retards crystallisation of the polymers. Due its large surface area the intensity of the peak abruptly increases in the composite electrolytes. No peak have appeared corresponding to the salt in the complexes, which confirms the amorphicity of the electrolytes. It illustrates that the polymer electrolytes have tend to be in amorphous phase

Conductivity Studies

A temperature dependent complex impedance plot of the electrolyte membrane with higher ionic conductivity [PEMA (19)-PC (67) - $LiClO_4$ (8) with 6 wt % of TiO_2] is shown in the Fig. 2.2. The measurements were done in the frequency range from 40 HZ to 300 KHZ at ambient temperature. The impedance studies were carried out by sandwiching the polymer electrolyte film between two stainless steel (SS) electrodes under spring pressure. The thickness of each sample was measured using a micrometer screw gauge..

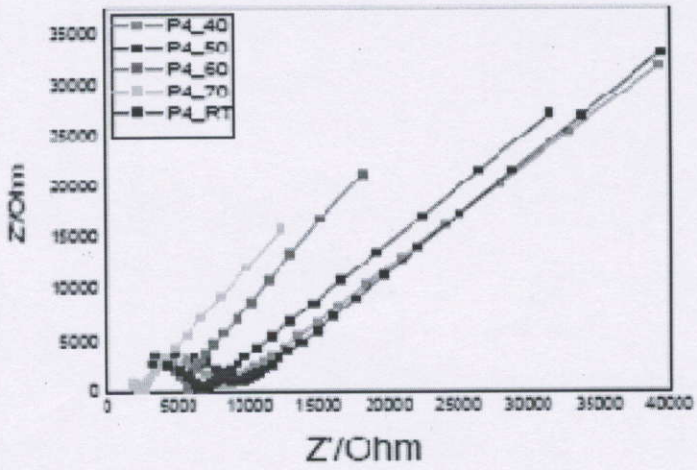

Fig. 2.2. Room temperature complex impedance plot of the prepared samples.

This plot shows linear spikes. The disappearance of the high frequency semicircular portion in the polymer complex impedance plot indicates that the current carriers are ions and the total conductivity is the result of ionic conduction. The bulk resistance of the electrolyte was measured by extrapolating an intercept of this plot on the real axis. The electrical conductivity of the electrolyte was calculated for the known values of bulk resistance (R_b), area (A) and the thickness (t) of the film using the formula:

$$\sigma = t / R_b A$$

Table 2.1

Ionic conductivity values of PEMA (19) + PC (67) + $LiClO_4$(8), X wt.% of TiO_2 in the total polymer weight

Sample coding	**PEMA(25)-TiO_2(X)-$LiClO_4$(8) _PC(67) Wt %**	**Ionic conductivity values (σ)×10^{-3} Scm^{-1} at different temperatures (K)**				
		303	**313**	**323**	**333**	**343**
P1	X=O	2.016	2.713	3.426	4.012	4.913
P2	X=2	2.312	3.026	3.812	4.423	5.162
P3	X=4	2.613	3.253	4.007	4.926	5.346
P4	X=6	2.903	3.621	4.287	5.396	6.102
P5	X=8	2.788	3.438	4.110	5.167	5.998

It has been seen that the addition of inorganic fillers leads to an increase in the ambient temperature conductivity upto 6 wt% of TiO_2 in the total polymer weight and then the ionic conductivity decreases due to higher concentration of ceramic fillers. Indeed, one may summarise that the presence of high dispersed particles in the polymer matrix may affect the crystallization rate by preventing the agglomeration of the polymer chains. Further, the particle size and content of the ceramic additive appear to be a critical factor. It is also seen that a reasonably high concentration of the filler is also necessary to affect the recrystallization rate of the polymer host.

Thermal Analysis

Thermal stability is an important parameter for acceptable performance during high temperature operation, which is related to safety concerns. In this work, the thermal stability of the polymer electrolytes was observed using thermo gravimetric analysis (TGA). The TGA curves indicates that the films of various ratio of filler TiO_2 exhibit weight loss and is mainly due to the presence of moisture which may be acquired during the loading of the sample or the evaporation of residual solvent.

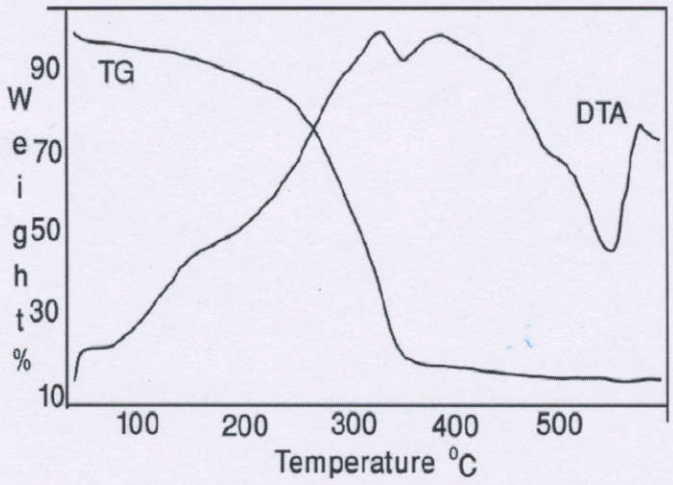

Fig. 2.3. TG/DTA analysis of TG/DTA traces of PEMA (19)-PC (67)-$LiClO_4$ (8) - TiO_2 (6 wt %)

Figure 2.3 shows the TG/DTA traces of PEMA (19)-PC (67)-$LiClO_4$ (8)-TiO_2 (6 wt %). The weight loss is also confirmed from the endothermic peaks observed at 120 °C in almost all the samples. All the prepared samples show appreciable weight losses of approximately 13, 23, 24 & 9% respectively at 250 °C-300 °C is primarily due to the degradation of Propylene Carbonate (PC)

because of the boiling point of the PC (242 °C). It may also be due to the blended polymer degradation.

An endothermic peak was observed at 65 °C and corresponding 7% of weight loss is attributed to the presence of moisture in the samples. The film starts decomposing at 222 °C followed by an endothermic peak, which indicates that the film is stable up to 222 °C. The DTA trace shows an endothermic peak around 416 °C, which corresponds to the melting point of PEMA polymer host. It is clear from these observations, that the PEMA based hybrid polymer electrolytes, which contain $LiClO_4$ as salt can be operated up to 222 °C.

Conclusion

PEMA based single polymer electrolyte have been investigated with the addition of PC as a plasticizer and TiO_2 as filler. The complexation of the prepared electrolyte systems was confirmed from XRD and FTIR analysis. X- Ray diffraction analysis revealed the semi crystalline nature of all the polymer electrolytes, which improves ionic conduction. All the electrolytes show appreciable conductivity at room temperature. Maximum conductivity 2.903×10^{-3} S cm^{-1} at room temperature with good mechanical stability has been observed for PEMA (19)-PC (67)-$LiClO_4$ (8)-TiO_2 (6 wt%). At 303K free standing nature was observed for PEMA/TiO_2/PC/$LiClO_4$ electrolyte film. From the TG-DTA observations it was noted that the electrolyte exhibited a maximum thermal stability of approximately 222 °C. In summary, polymer blend electrolytes with possible applications in high-energy density batteries have been identified in terms of such parameters as conductivity and thermal stability.

C. Preparation of polymer electrolyte films

The specific amount of PVdF-HFP, PEMA with inorganic salt $LiN(CF_3SO_2)_2$ and plasticizer of each composition were weighted and PEMA were taken in a relative density bottle and kept inside the vacuum heating arrangement and heated up to 100 °C for nearly 10 hours respectively. Then the inorganic salt was heated by the same procedure upto 100 °C for nearly 10 hours. In this work, distilled acetone was used as a solvent. PVdF-HFP, PEMA, $LiN(CF_3SO_2)_2$ with different plasticizers were dissolved in acetone separately. After their dissolution, they were mixed together in a conical flask.

The conical flask which contains polymer-salt complex was placed on the top of the magnetic stirrer arrangement. The mixture was stirred for about 24 hours at room temperature. Then it was heated to 60 ^{o}C and stirred for one hour at the same temperature. At the end of the stirring process, the mixture coagulated into a gel like formation. The slurry thus obtained was poured into a round Teflon die of 2 cm which has a piston like arrangement at the centre. The movable centre piston can be pushed from the bottom by applying a little finger pressure so that the piston arrangement can move up. The polymer films were dried under argon atmosphere at room temperature for 24 hours in order to evaporate the presence of residual solvents in the polymer films. This procedure provided mechanically stable, free standing and flexible films. The prepared polymer films of thickness 0.1 to 1 mm were obtained

Structural Analysis

The X-ray diffractograms shown in Fig.3.1 suggest that the sample of this study exhibit the co-existence of a multiphase system, which means that the polymer matrix possesses crystalline PVdF and amorphous HFP regions simultaneously. This can be due to a confirmation of partial crystallization of PVdF units in the copolymer which gives a semi-crystalline structure of P(VdF-HFP). In order to investigate the effect of various plasticizers (EC, PC, DEC, DMC, GBL) - $LiN(CF_3SO_2)_2$ system XRD analysis has been performed. The characteristic diffraction peaks of the P(VdF-HFP) at angles 18.09 and 20.47^{o} is reduced upon the addition of the plasticizers and lithium salt. The diffractograms in Fig.3.1 (d-h) reveals that the amorphous nature is predominant in the complex which is due to the addition of plasticizers. The maximum conductivity value 6.39×10^{-3} Scm^{-1} is obtained for EC Fig.3.1 (e) based complex which is in accordance with the lower degree of crystallinity as compared to the four systems developed.

The peaks observed for 2θ values around 16.5^{o} for pure PEMA disappear in complexed polymer films. The presence of broad humps in the pattern for PEMA confirms the amorphous nature of the polymer. The diffraction pattern of $LiN(CF_3SO_2)_2$ shows intense peak at angles at 2θ=13.6, 15.9, 18.9 and 21.4^{o} which reveals the crystalline nature of the ionic salt. Most of the peaks pertaining to $LiN(CF_3SO_2)_2$ disappeared in the complexes, which indicates the complete dissolution of the salt in the polymer matrix.

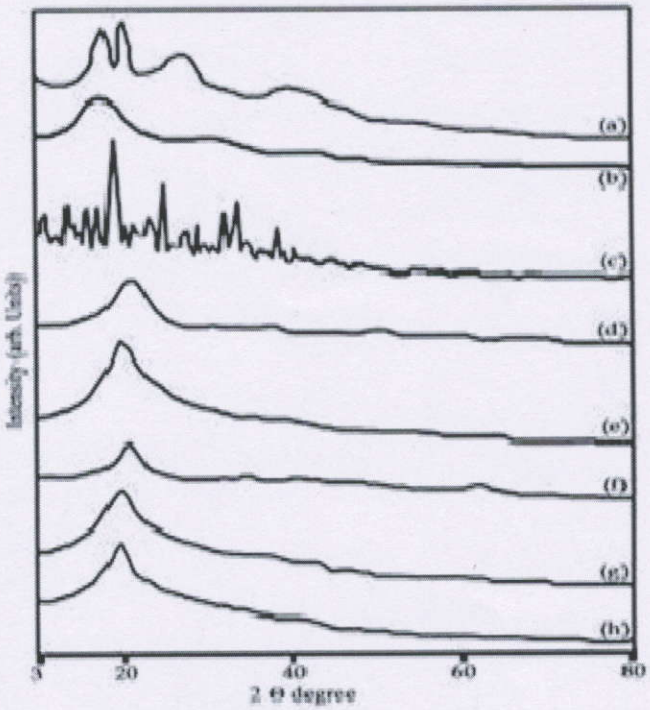

Fig. 3.1. XRD Patterns of pure (a) PVdF-HFP (b) PEMA (c) $LiN(CF_3SO_2)_2$ (d) PVdF-HFP - PEMA - $LiN(CF_3SO_2)_2$ - DEC (e) PVdF-HFP - PEMA - $LiN(CF_3SO_2)_2$ – EC (f) PVdF-HFP - PEMA - $LiN(CF_3SO_2)_2$ – DMC (g) PVdF-HFP - PEMA - $LiN(CF_3SO_2)_2$ - PC (h) PVdF-HFP - PEMA-$LiN(CF_3SO_2)_2$- GBL

Complexation Studies

FTIR is an important tool for investigating polymeric structure that provides information about the interaction/ complexation between the various constituents in the polymeric film. In order to understand the interactions between Li^+ ions and the polymer hosts in the polymeric electrolytes, the IR spectra of pure materials, polymer-salt and polymer-salt-plasticizer samples are presented. The FTIR spectra of pure PEMA, PVdF-HFP, $LiN(CF_3SO_2)_2$ and EC, PC, DMC, DEC and GBL based complexes are shown in Fig.3.2 (a-h) respectively.

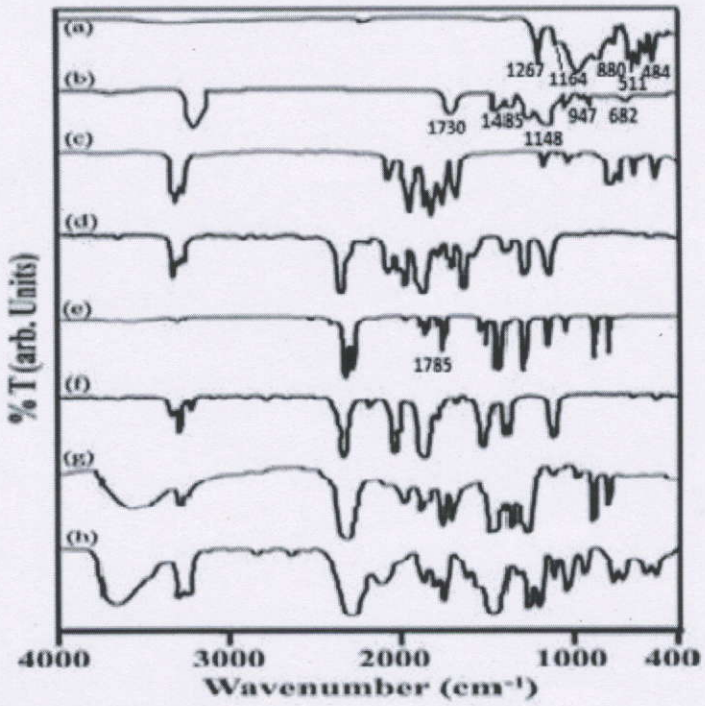

Fig. 3.2. FTIR Spectra of pure (a) PVdF-HFP (b) PEMA (c) $LiN(CF_3SO_2)_2$ (d) DEC (e) EC (f) DMC (g) PC (h) GBL.

FTIR spectra were recorded in the transmittance mode. The crystalline phase of the PVdF-co-HFP polymer is identified by the Vibrational bands at 511 and 484cm^{-1} are assigned to the bending and wagging vibrations of $-CF_2$ respectively. The crystalline phase of the PVdF-co-HFP polymer is identified by the Vibrational bands at 1164 and 1267cm^{-1} are assigned to the symmetrical stretching of $-CF_2$ and –CF groups respectively. The peak at 880 cm^{-1} is assigned to the vinylidene group of the polymer. Spectrum of PEMA shows Vibrational peaks at 2983 and 2940cm^{-1} which are ascribed to the asymmetric and symmetric C-H stretching of the methylene group of PEMA respectively. The absorption peak of PEMA at 1730cm^{-1} is assigned to the C=O carbonyl group. The Vibrational peaks corresponding to the $-CH_2$ scissoring, $-CH_2$ wagging and $-CH_2$ rocking are observed at 1485, 947 and 756 cm^{-1} respectively. The C-H bonding due to $C=CH_2$ group is observed at 939cm^{-1}. Some other carboxylic acid ester groups were observed as broad features at 1148cm^{-1}.

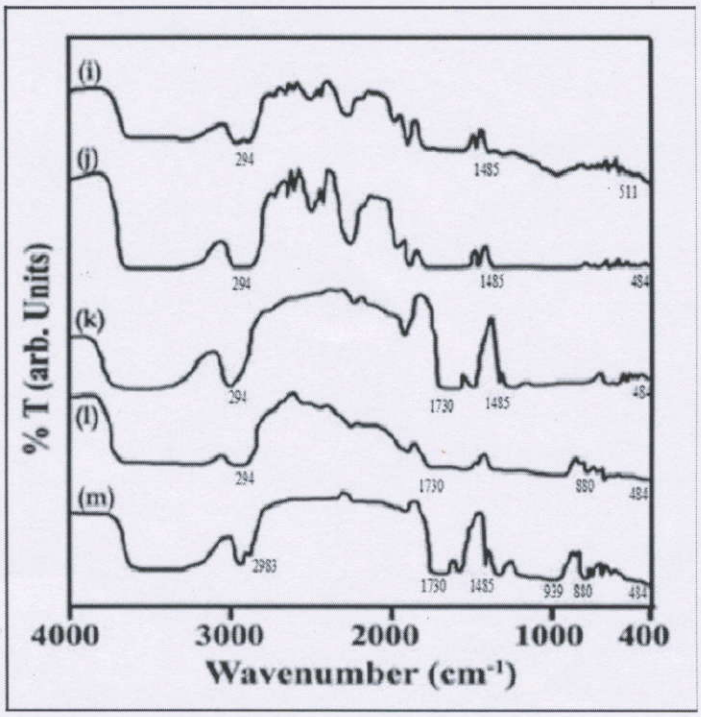

Fig. 3.2. FTIR Spectra of complexes (i) PVdF-HFP - PEMA - $LiN(CF_3SO_2)_2$ – DEC, (j)PVdF-HFP - PEMA - $LiN(CF_3SO_2)_2$ – EC (k)PVdF-HFP - PEMA - $LiN(CF_3SO_2)_2$ –DMC (l)PVdF-HFP - PEMA - $LiN(CF_3SO_2)_2$ – PC (m)PVdF-HFP-PEMA - $LiN(CF_3SO_2)_2$- GBL.

The spectra of the samples containing plasticizers in the polymer salt complexes are shown in Fig.3.2 However the C=O bonds in EC (1785 cm^{-1}) seems to have overlapped and broadened Fig.3.2(j). This may be due to the association through the redistribution of charge accompanying the formation of ionic pair increases aggregation. This is attributed to the carbonyl group (C=O) and oxygen atoms in the EC ring. The broadening of the C=O band in the plasticized polymer salt complexes indicates that the plasticizer just interacts physically with the polymer and the salt. No chemical reaction occurred between the plasticizer and polymer or between the polymer and to the salt.

With the addition of lithium salts to PEMA, the C=O stretching band broadened and shifted to lower wave numbers. This indicates that there is an interaction between the carbonyl group of ester and lithium salts via a coordinate bond and hence complexation has occurred. To justify the co-ordination of the lithium salt, the FTIR spectra of pure $LiN(CF_3SO_2)_2$ was observed. The $LiN(CF_3SO_2)_2$ ion has a vibrational spectrum, which is very sensitive to its state of coordination, producing a series of different IR bands as its environment changes. The peak

appearing at wave numbers 1333 and 1142cm^{-1} are due to the S=O asymmetric stretch and C-F stretch. This seems to have disappeared in the complexes which confirmed that interaction has occurred. The O-CH_3 asymmetric stretch bands of PEMA at 1433 cm^{-1} are found to exist at the same wave numbers in the complexes and in pure PEMA. This indicates the co-ordination to the salt did not occur at these groups. By comparing the band spectra of pure polymers and complexes, it is apparent that the band assignments are shifted in the FTIR spectra. In addition, some new peaks are present and some disappear in the complexes. Thus the spectral analysis confirms the complexation of PVdF-co-HFP and PEMA polymer, plasticizers and lithium salts.

Conductivity Studies

The ionic conductivity of the polymer electrolytes mainly depends on the actual concentration of conducting species and their mobility. Two semicircles should appear in the impedance spectrum for a symmetric cell i.e. one at high frequencies corresponding to the bulk electrolyte impedance and the other at low frequencies related to the interfacial impedance. The high-frequency semicircle does not appear in practical impedance plots for plasticized polymer electrolyte membranes. This feature indicates that the conductivity is mainly due to ions.

The room temperature conductivity of the polymer electrolytes are measured by knowing the values of the bulk resistance R_b, area A and thickness l of the film by applying the equation $\sigma = l/R_b A$. The impedance curves of EC based PEMA,PVdF-HFP,$LiN(CF_3SO_2)_2$ system are shown in the Fig. 3.3 for the temperature range of 303-343K.

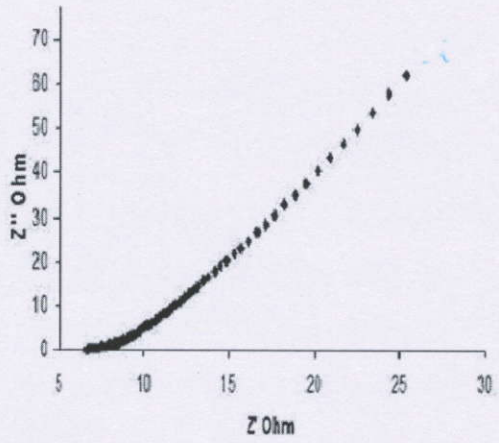

Fig. 3.3. Z real Vs Z imaginary plot for PVdF-HFP - PEMA- $LiN(CF_3SO_2)_2$- EC at room temperature.

The high frequency response yields information about the properties of electrolyte. The low frequency response carries information about the electrode/ electrolyte interface. It is observed that as the temperature increases, the conductivity also increases for all complexes.

The effect of the plasticizer on the polymer mobility and conductivity depends on the specific nature of the plasticizer including viscosity, dielectric constant, polymer-plasticizer interaction, ion plasticizer co-ordination, structure and molecular weight. The plasticizer with low viscosity provides ionic pathways for the migration of free Li ions. The high dielectric constant of the plasticizer helps in an increase in the salt dissociation.

Table 3.1.

Conductivity values of PVdF-HFP (20) - PEMA (5) - $LiN(CF_3SO_2)_2$ (8) - X (67) [where X = DEC, EC, DMC, PC & GBL] at different temperatures.

Films	**X**	**Conductivity values of PVdF-HFP - PEMA - $LiN(CF_3SO_2)_2$ – X in Scm^{-1}**				
		303 K	**318 K**	**333 K**	**353 K**	**373 K**
A_1	DEC	1.22×10^{-5}	3.81×10^{-5}	7.51×10^{-5}	9.66×10^{-5}	2.23×10^{-4}
A_2	EC	6.39×10^{-3}	1.12×10^{-2}	2.49×10^{-2}	5.94×10^{-2}	9.69×10^{-2}
A_3	DMC	7.52×10^{-5}	1.18×10^{-4}	1.96×10^{-4}	3.64×10^{-4}	4.23×10^{-4}
A_4	PC	3.17×10^{-3}	4.90×10^{-3}	9.55×10^{-3}	2.69×10^{-2}	3.54×10^{-2}
A_5	GBL	1.48×10^{-4}	2.70×10^{-4}	6.00×10^{-4}	1.26×10^{-3}	3.02×10^{-3}

From Table 3.1, it is observed that the complex PEMA, PVdF-HFP-$LiN(CF_3SO_2)_2$-EC shows a maximum conductivity value of 6.39×10^{-3} Scm^{-1} at 303K as compared to other prepared gel electrolytes which is mainly due to the higher dielectric constant (89.6 at 40°C) of Ethylene carbonate. The conductivity is obtained in the decreasing order of EC, PC, GBL, DMC and DEC based electrolytes which are in accordance with their dielectric constants 89.6, 64.4, 39.1, 3.12 and 2.82 at 40°C.These results are in accordance with those reported earlier using different plasticizers like EC, PC, GBL, DMC and DEC.

The variation of log conductivity verses inverse absolute temperature of the developed complexes is given in Fig.3.4. From the plot it is observed that as temperature increases the conductivity also increases for all compositions. The non-linearity in the plot indicates that the ionic transport in polymer electrolytes is dependent on polymer segmental motion. This can be explained on the basis of VTF relation. It supports the idea that, ionic transport may be expected to take place along the plasticizer- rich phase which act as a tunnel for ionic transport.

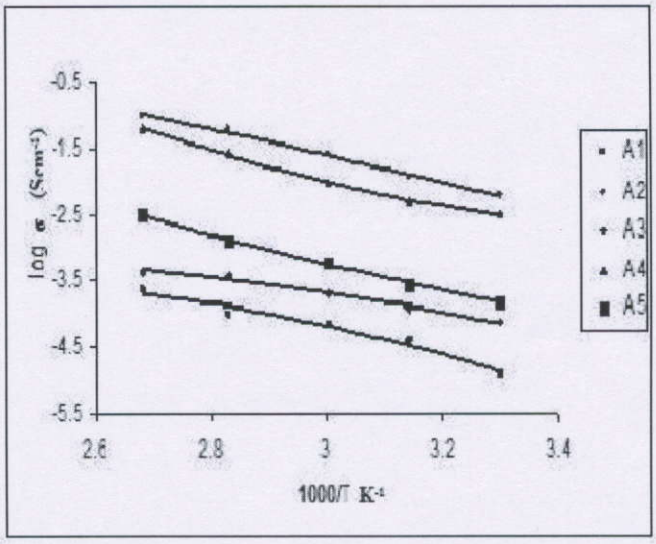

Fig.3.4. Arrhenius plot of log σ versus 1000/T for PVdF-HFP - PEMA - $LiN(CF_3SO_2)_2$ – X [where X = DEC,EC, DMC, PC & GBL]

Morphological Analysis

The analysis of microstructure of the polymer electrolyte plays an important role in determining the structure, spatial arrangement of atoms or molecules in the electrolytes. In polymer blends, the domain size depends on a number of factors including the type of solvent and its evaporation rate and polymer, plasticizer, salt interactions. However, the size of the dispersed domain is largely governed by the level of polymer compatibility.

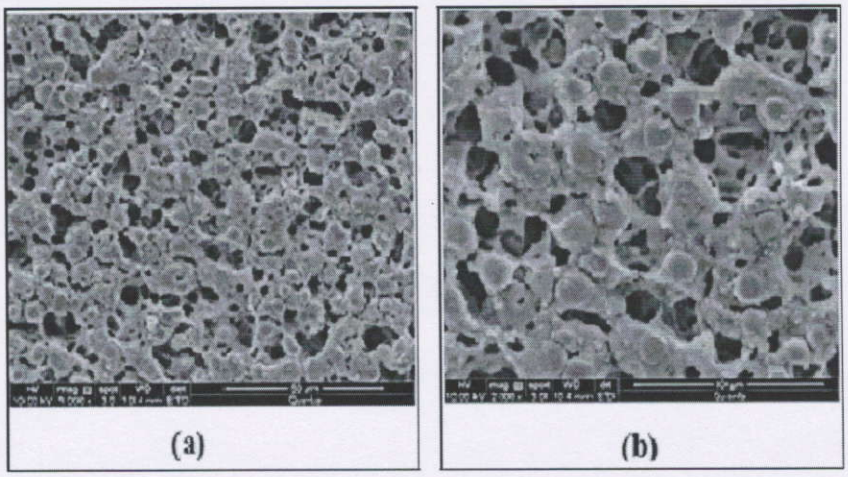

Fig. 3.5. SEM micrographs of PVdF-HFP - PEMA - $LiN(CF_3SO_2)_2$ - EC at 1000 & 2000 magnifications.

Scanning electron micrographs (SEM) of the polymer electrolyte film with maximum conductivity are shown in Fig. 3.5 (a & b) at 1000 and 2000 magnifications. It is evident from the figure that the surface of the film shows highly porous structure. These pores are responsible for the entraption of plasticizer which could be responsible for the higher conductivity of the polymer electrolyte (film A_2). Further, it is confirmed that the amorphous nature of the electrolyte is increased due to the addition of salt and plasticizer.

Conclusion

Plasticized polymer electrolytes comprising PC, EC, DMC, DEC and GBL complexes with PVdF-HFP (20)– PEMA (5) – $LiN(CF_3SO_2)_2$ (8) system are prepared using solvent casting technique. The structure and complexation of the developed polymer electrolytes have been confirmed using XRD and FTIR studies. The addition of plasticizer into the complexes reduced the peak intensity of the blended polymer electrolytes. The maximum conductivity value has been obtained for EC based complex because of their higher dielectric constant as compared to the other plasticizers studied. The maximum conductivity obtained at 303 K is 6.39×10^{-3} Scm^{-1}. The surface morphology of the developed films is analyzed by scanning electron microscope.

D. **Preparation of polymer electrolyte films**

The nano composite polymer electrolytes were prepared by solution casting technique. Poly (ethyl methacrylate) (PEMA MW 515,000), Propylene carbonate (PC), Lithium perchlorate salt ($LiClO_4$) and MWCNT were obtained from sigma Aldrich, USA. The solvent tetrahydrofuran (THF) from SRL, Mumbai were used as received. The appropriate quantities of polymer and salt were dissolved separately in THF and then mixed together with plasticizer and filler. The solution was stirred continuously for 24 hrs to obtain a homogeneous mixture and then it was allowed to evaporate THF slowly until jelly state was achieved. The jelly solution was cast on to the glass plate and the obtained free standing films were further dried at 60°C for 12 hrs to remove the residual traces of THF. The structural studies of the electrolytes were carried out by X-ray diffractometer (X'pert PROPANalytical). The prepared electrolyte were subjected to an ac impedance analysis, in order to calculate the ionic conductivity with the help of stainless steel blocking electrodes using a computer controlled μ-autolab type III potentiostat/Galvanostat in the frequency range 100Hz to 300KHz.

Structural Analysis

XRD patterns of pure and complexed PEMA films with various fractions of MWCNT are shown in the fig 4.1.

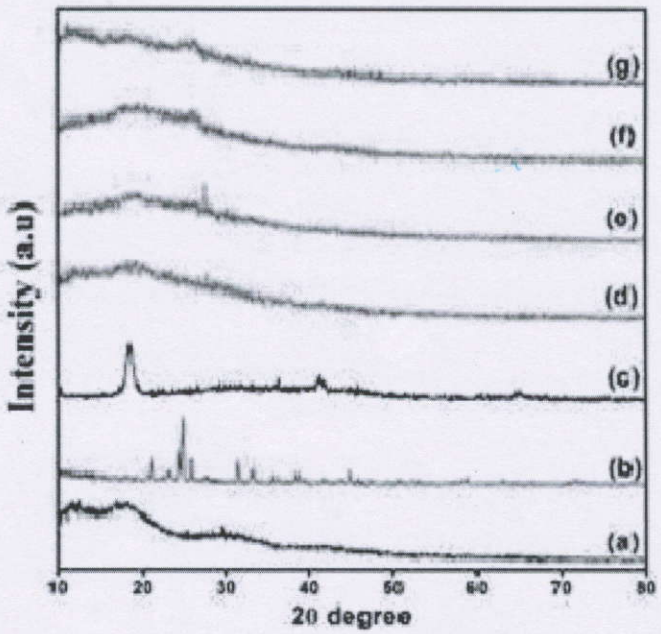

Figure 4.1. XRD patterns of (a) PEMA, (b) $LiClO_4$, (c) MWCNT and polymer complexes (d-g).

The presence of broad humps in the pattern for PEMA confirms the amorphous nature of the polymer. The peak observed for 2θ values around 18.6° for pure PEMA disappeared in complex polymer films. MWCNT at 10°, 26°, 30°, 46° corresponding to (111), (100), (110), (222) planes observed in pattern (c) were absent in pattern (d-g) which suggested that MWCNT were well surrounded and dispersed within the PEMA matrix. However the characteristic peaks corresponding to the MWCNT are impervious from its position. It is observed from the fig (d-g) that the characteristic peaks corresponds to $LiClO_4$ are mislaid in the complexes confirmed the absolute dissolution of the salt in the polymer matrix. This reduction in crystallinity upon the addition of filler is attributed to smaller particles of inert fillers which changes the chain re-organization and facilitates for higher ionic conduction.

Conductivity Studies

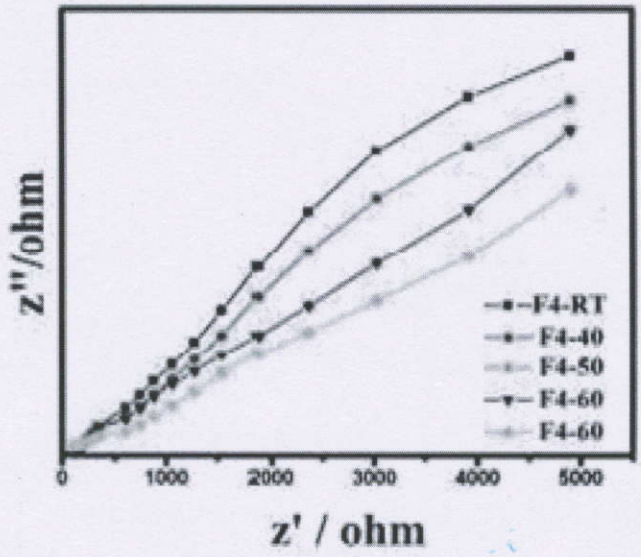

Figure 4.2. Maximum conductivity of [PEMA (19wt%), $LiClO_4$ (8 wt%), PC (67 wt%)] with 6 wt% of MWCNT at different temperatures

This Impedance spectroscopy is a method to characterize the electrical properties of materials and their interfaces with electrically conducting electrode. Fig. 4.2 represents the typical impedance plot of PEMA composite polymer electrolyte with propylene carbonate (PC) as plasticizer. The ionic conductivity of the polymer electrolyte was calculated from the measured bulk resistance (R_b) for the known area and the thickness (l) of the polymer film using the formula $\sigma = l/R_bA$. The room temperature complex impedance plot of the nanocomposite polymer electrolyte with different concentrations of MWCNT is given in table 4.1.

TABLE 4.1. Temperature dependent ionic conductivity values of the prepared samples.

Code	PEMA (19)-$LiClO_4$(8)-	Conductivity values (σ) Scm^{-1} at different temperatures				
		303K	313K	323K	333K	343K
F1	X=0	$8.64X10^{-7}$	$9.67X10^{-7}$	$9.90X10^{-7}$	$1.01X10^{-6}$	$1.01X10^{-6}$
F2	X=2	$4.72X10^{-5}$	$4.92X10^{-5}$	$5.17X10^{-5}$	$5.23X10^{-5}$	$5.50X10^{-5}$
F3	X=4	$7.76X10^{-4}$	$8.83X10^{-4}$	$8.89X10^{-4}$	$9.42X10^{-4}$	$9.93X10^{-4}$
F4	X=6	$1.17\ X10^{-3}$	$1.19\ X10^{-3}$	$2.97\ X10^{-3}$	$3.62\ X10^{-3}$	$4.98\ X10^{-3}$

The maximum ionic conductivity corresponding to lowest bulk resistance [PEMA (19), $LiClO_4$ (8), PC (67 wt%)] with 6 wt% of MWCNT obtained was 1.171×10^{-3} Scm^{-1}. The increase in conductivity may be due to filler particles acting as nucleation centers for the formation of minute crystallites & formation of the new kinetic path via polymer - filler boundaries.

Temperature dependence of ionic conductivity

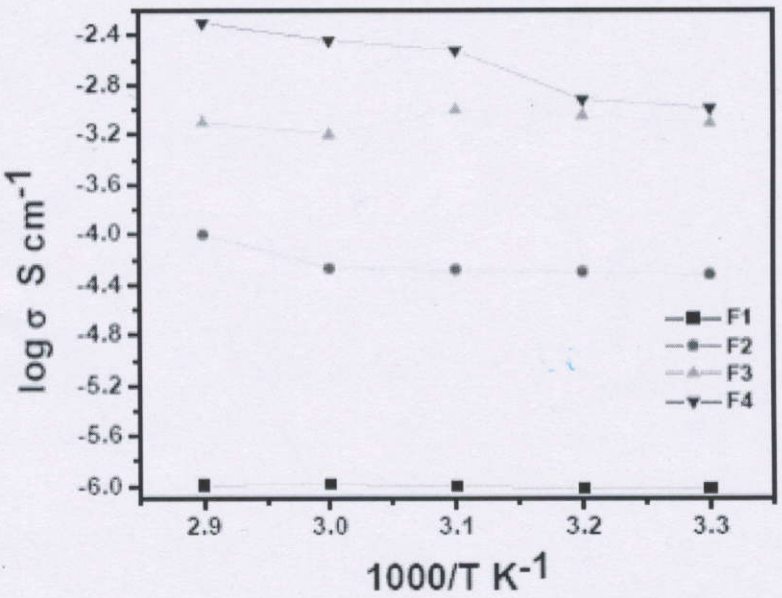

Figure 4.3. Temperature dependent ionic conductivity plot of the prepared samples.

It has been observed that as the temperature increases the ionic conductivity also increases for all the polymer electrolytes. The variations of log with the inverse of the absolute temperature for all prepared electrolyte films are shown in Fig. 4.3. The temperature dependent ionic conductivity plot seems to obey the Vogel-Tamman-Fulcher (VTF) relation,

$\sigma = AT^{-1/2}\exp(-B/(T-T_o))$, where A is proportional to the number of charge carriers, T_0 is the temperature at which the conductance tends to zero and B is the activation energy. The dependence of the ionic conductivity of the polymer electrolyte on temperature describes the transport properties in a viscous matrix. The change of conductivity with temperature is due to segmental motion, which results in an increase in the free volume of the system. The free volume around the polymer chain causes the mobility of ions and hence the conductivity increases from the table it is understood,as the temperature varies the composite film exhibits higher conductivity value of the order of 10^{-3} Scm^{-1} at 303K.

Conclusion

PEMA based composite polymer electrolyte complexed with 6 wt% MWCNT looks desirable and promising for lithium battery applications. Since the highest ionic conductivity at room temperature 1.171 x 10^{-3} Scm^{-1} was observed for the system [PEMA (19wt %), $LiClO_4$ (8wt %), PC (67wt %)] with 6 wt% of MWCNT.

E. **Preparation of polymer electrolyte films**

PVC (average Mw ~ 534,000) and PEMA (average Mw ~ 515,000) were purchased from Aldrich and dried under vacuum at 80 °C for 24 hours. Reagent grade anhydrous Lithium perchlorate ($LiClO_4$) was used after drying in vacuum at 110 °C for 24 hours. The plasticizer propylene carbonate (PC) (from Aldrich) was used as supplied. The nanosized TiO_2 (<100 nm particle size) was purchased from Aldrich and used as a ceramic filler. All the electrolytes have been prepared by the solvent casting technique. Appropriate quantities of PVC, PEMA, and $LiClO_4$ are dissolved by adding them in sequence to tetrahydrofuran (THF) and stirred for 24 hours. The resulting solution is poured onto a glass plate, and the THF is allowed to evaporate in air at room temperature for several hours. The films are further dried at 60°C for 24 hours in vacuum to remove any traces of THF.

Structural Analysis

X-ray diffraction patterns of pure PVC, PEMA, $LiClO_4$, and PVC (5)–PEMA (20)–PC (67)-$LiClO_4$ (8) polymer electrolyte with X% of TiO_2 (where X = 0, 5, 10, 15, 20) are shown in Fig. 5.1.

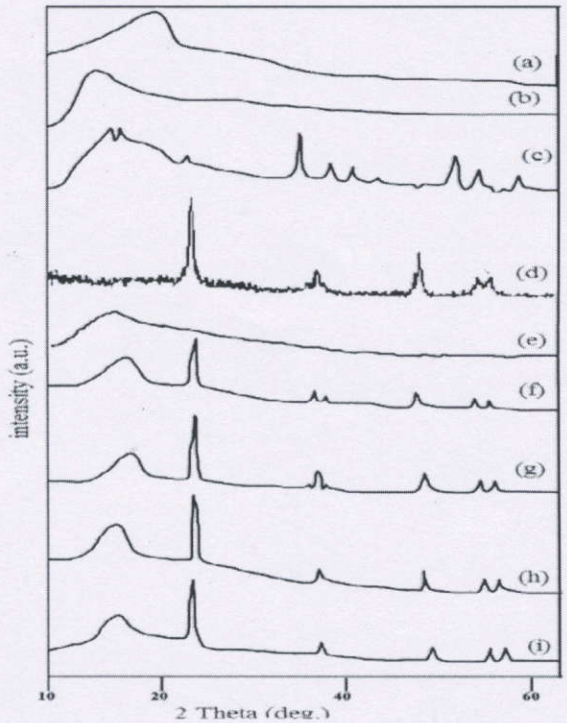

Figure 5.1. X-ray diffraction patterns of (a) Pure PEMA, (b) Pure PVC, (c) Pure $LiClO_4$, (d) Pure TiO_2, (e) PVC (5)-PEMA (20)-$LiClO_4$ (8)-PC (67)-TiO_2(0), (f) PVC (5)-PEMA (20)-$LiClO_4$ (8)-PC (67)-TiO_2(5), (g) PVC (5)-PEMA (20)-$LiClO_4$ (8)-PC (67)-TiO_2(10), (h) PVC(5)-PEMA(20)-$LiClO_4$(8)-PC(67)-TiO_2(15), (i) PVC(5)-PEMA(20)-$LiClO_4$(8)-PC(67)-TiO_2(20).

It is clear that both polymers are amorphous in nature because no sharp crystalline peaks are observed.The diffraction peaks appearing at 2θ values 18^o and 23^o indicate the crystalline phase of $LiClO_4$ in Fig. 5.1(c). The peaks corresponding to $LiClO_4$ were not observed in the Fig. 5.1(e-i), indicating that the $LiClO_4$ does not remain as a separate phase in the polymer electrolyte system which confirms the complete dissociation of $LiClO_4$ in the polymer matrix.The characteristic peaks at $2\theta = 13^o$ for PVC and 18.6^o for PEMA are revealed from Fig. 5.1(a) and 5.1(b), respectively. The diffraction peak of PEMA is markedly reduced in all the complexes. The shift and decrease in the relative intensity of the peaks suggest that complexation has occurred between the salt and the polymers. The analysis shows that the nature of diffraction patterns of pure samples significantly changed due to the disturbances in the ordered arrangement of polymer side chains when they are blended. This indicates that the salt, $LiClO_4$, most likely blends with PVC/PEMA polymer blend at the molecular level and gives a clear indication of complexation of the salt in the polymer blend system. The obtained amorphous phase of polymer blend in the

electrolyte membrane enhances higher ionic conduction, meanwhile the crystalline phase of the filler provides strong mechanical support in the polymer electrolyte. We can observe that the position of the sharp peak coincided with a peak at $2\theta = 25.2^{o}$ and 48^{o} from the X-ray scans of pure TiO_2 in Fig. 5.1(d). This confirms the presence of TiO_2 crystallites within the polymer matrix. On the other hand, the spectrum of PVC/PEMA films containing TiO_2 showed a sharp peak at $2\theta = 25.2^{o}$, showing $W \geq 5wt\%$ can cause structural variations in the polymeric network. The nano sized TiO_2 dispersed emulsion can penetrate the space between the polymer chains, and consequently the homogeneously dispersed ceramic filler in the matrix prevents or retards crystallization of the polymers due to its large surface area. The intensity of the peaks abruptly decreases in the composite electrolytes. No peaks appeared corresponding to the salt in the complexes, which confirms the amorphous nature of the electrolytes.

Complexation Studies

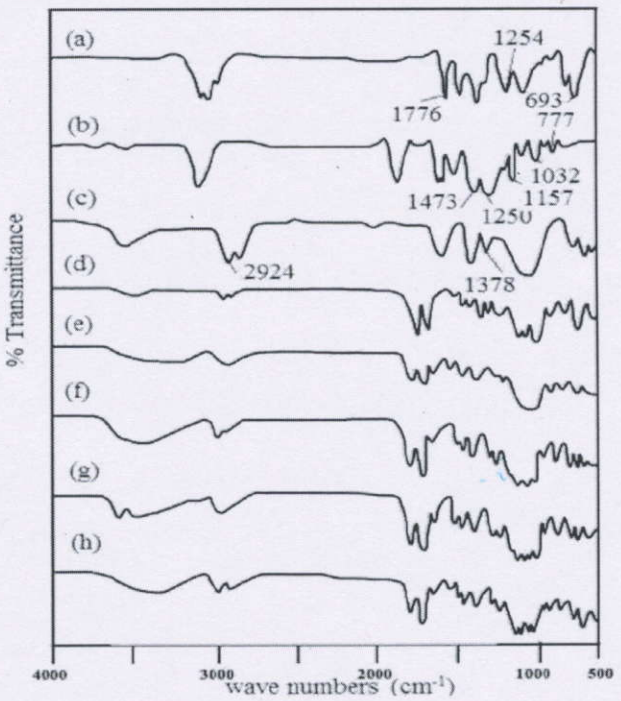

Figure 5.2. FTIR spectra of (a) Pure PVC (b) Pure PEMA (c) $LiClO_4$, (d) PVC (5)-PEMA (20)-$LiClO_4$ (8)-PC (67)-TiO_2(0), (e) PVC (5)-PEMA (20)-$LiClO_4$ (8)-PC (67)-TiO_2(5), (f) PVC (5)-PEMA (20)-$LiClO_4$ (8) -PC (67)-TiO_2(10), (g) PVC(5)-PEMA(20)-$LiClO_4$(8)-PC(67)-TiO_2(15), (h) PVC(5)-PEMA(20)-$LiClO_4$(8)-PC(67)- TiO_2(20)

FTIR spectra of composite polymer complexes are shown in Fig. 5.2. The peak at 1725 cm^{-1} represents the carbonyl stretching vibration of PEMA. In PEMA, the peaks at 2982, 2939, and 2910 cm^{-1} are due to the methylene (C) CH_3 and ethylene (O) C_2H_5 groups which overlap. Peaks at 2963 and 1329 cm^{-1} are assigned respectively to asymmetric C-H methylene group vibration and in-plane CH deformation of PVC. Further, the peaks at 954 and 630 cm^{-1} are assigned to trans CH rocking and *cis*-CH wagging of PVC. The peak at 1777 cm^{-1} represents the CH_3-C- vibration of propylene carbonate. The frequency of C=O at 1785cm^{-1} indicates the interaction of the plasticizer with $LiClO_4$. The weak intensity peak appearing at 507 cm^{-1} is assigned to the stretching mode of ClO_4^-. The vibrational peaks at 1776, 1254, 959, 847, and 693 cm^{-1} of pure PVC, 1473, 1250, 1157, 1032, and 777 cm^{-1} of pure PEMA, 2924 and 1378, cm^{-1} of pure $LiClO_4$, and 1650 cm^{-1} of pure TiO_2 shifted to 1789, 1266, 972, 861, 713, 1482, 1266, 1173, 1025, 792, 2936, 1389, and 1660 cm^{-1}, respectively. It is also found that some of the peaks appearing in the pure polymers and salts disappeared in the complexes, such as 2910, 1807, 1400, 10 87, 923, and 632 cm^{-1}. In addition to this, a few new peaks are observed at 1532, 1142, and 1173 cm^{-1} in polymer complexes. The shifting of peaks and formation of new peaks in electrolyte systems suggests the polymer-salt interaction in PVC/PEMA blend based composite polymer electrolytes.

Conductivity Studies

Fig. 5.3 shows the complex impedance plot of PVC (5)-PEMA (20)-PC (67)-$LiClO_4$ (8) with 15 wt% of TiO_2 at various temperatures. The plot shows linear spikes. The disappearance of the high frequency semicircular portion in the polymer complex impedance plot indicates that the majority of the current carriers in the electrolyte medium are ions and that the total conductivity is mainly due to ion conduction. The bulk resistance of the electrolyte was measured by extrapolating the intercept of this plot on the real axis. The electrical conductivity of the electrolyte was calculated for the known values of bulk resistance (Rb), area (A), and the thickness (l) of the film using the formula $\sigma = l/RbA$. The conductivity values obtained for the polymer electrolyte increases with temperature and ceramic concentration. This may be due to the availability of ions throughout the ceramic-rich phase which entraps the residual solvents, increasing ion mobility. The conductivity is not a linear function of filler concentration. The increase in conductivity has been attributed to the ceramic particles acting as a nucleation centers for the formation of minute

crystallites of the ceramic particles in the formation of amorphous phase in the polymer electrolyte and to the formation of a new kinetic path *via* polymer-ceramic boundaries. Hence, ceramic plays a dual role, *i.e.* enhancement of ionic conductivity up to a particular concentration, above which it acts as the hindering agent to conductivity.

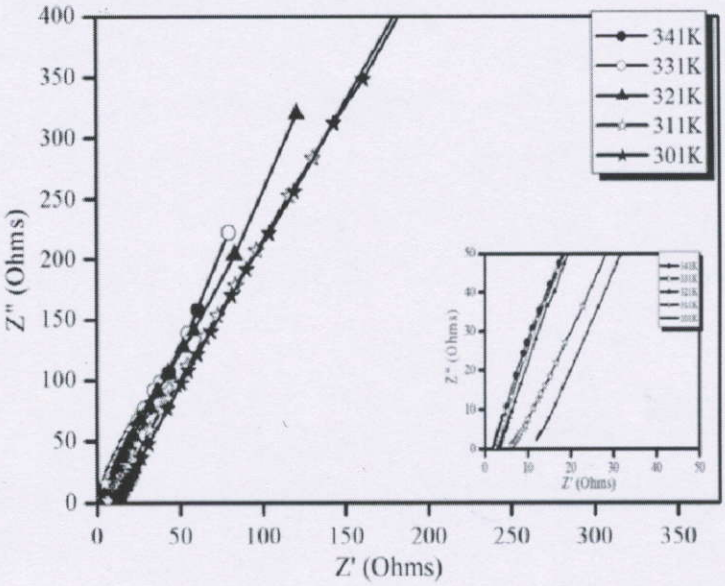

Figure 5.3. Impedance diagram for PVC(5)-PEMA(20)-$LiClO_4$(8) -PC(67)-TiO_2(15) wt% at various temperatures

Table 5.1. Ionic conductivity values for PVC(5)-PEMA(20)-PC(67)-$LiClO_4$(8)-TiO_2(X wt%) (where X = 0, 5, 10, 15, 20) system

Film	TiO_2 ratio	Ionic conductivity ($\times 10^{-3}$ S cm^{-1})				
		301 K	311 K	321 K	331 K	341 K
E1	0	3.454	3.878	4.043	4.578	5.588
E2	5	4.352	5.142	7.915	9.124	12.232
E3	10	5.812	7.784	11.175	11.782	13.415
E4	15	7.179	9.476	11.794	13.102	14.214
E5	20	6.426	8.079	11.326	12.156	13.962

From Table 5.1, it is seen that the addition of inorganic fillers leads to an increase in the ambient temperature conductivity up to 15 wt% TiO_2, and then the ionic conductivity decreases with increasing concentration of ceramic fillers. At low concentration levels, the dilution effect

which tends to depress the conductivity is efficiently countered by the specific interactions of the ceramic surface, which promotes fast ion transport. Thus, the net result is a progressive enhancement of the conductivity. At higher filler content, the dilution effect predominates and the conductivity decays. It is found that the PVC-PEMA-$LiClO_4$-PC complex with 15wt% TiO_2 has the maximum room temperature conductivity of 7.179×10^{-3} S cm^{-1} which is higher compared to the system bereft of ceramic addition. Irrespective of the reasoning, it can safely be assumed that as the T_g decreases, the less ordered amorphous phase region becomes flexible, resulting in increased segmental motion of the polymer chains as reflected by enhanced conductivity.

However the conductivity is found to decrease after an optimum concentration is attained; on further addition of filler a continuous non-conductive phase built up by a large amount of filler blocks up lithium-ion transport, resulting in an increase in total resistance of the composite polymer electrolyte. It is reported for many composite polymer electrolytes formed by the addition of filler that ion conductivity increases to a maximum value at 5wt%-15wt% of filler. The result reveals that the addition of small particle size ceramic powders enhances the degree of amorphicity of the polymer electrolyte. Further, the particle size and content of the ceramic additive appear to be a critical factor. It is also seen that a reasonably high concentration of the filler is also necessary to affect the recrystallization rate of the polymer host. The temperature dependence of the ionic conductivity of PVC(5)- PEMA(20)- PC(67)- $LiClO_4$(8)- X% of TiO_2 (where X = 0,5,10,15,20) in the total polymer electrolyte is shown in Fig. 5.4.

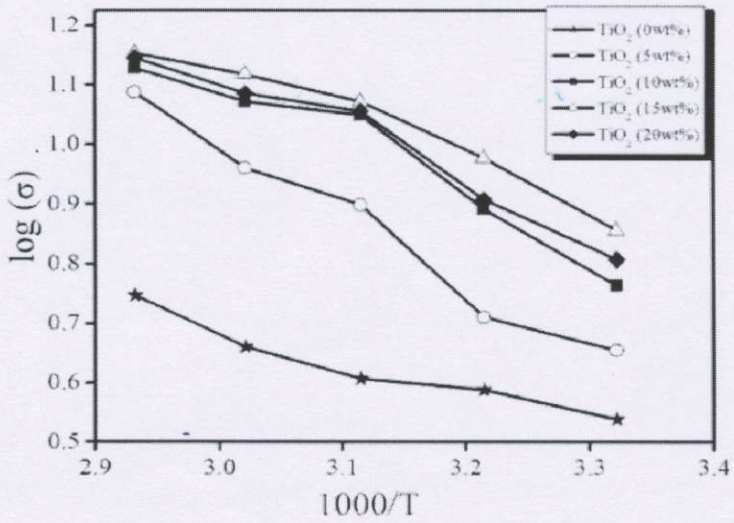

Figure 5.4. Arrhenius plot of PVC(5)-PEMA(20)-$LiClO_4$(8)-PC(67)- TiO_2(X wt%) (where X = 0, 5, 10, 15, 20) composites

From the plot it has been observed that as temperature increases the conductivity values also increase for all the compositions. The non-linearity in Arrhenius plots indicates that ion transport in polymer electrolytes is dependent on polymer segmental motion. The curved behavior of the plots suggests that the data can be better described by the Vogel–Tamman–Fulcher (VTF) relation, which describes the transport properties in a viscous matrix. This supports the idea that the ion moves through the plasticizer-rich phase.

Thermal Analysis

The thermal stability of the polymer electrolyte has been studied for its use in practical applications because thermal stability is an important parameter for guaranteeing acceptable performance during high temperature operating which is related to safety concerns. In this work, the thermal stability of the polymer electrolytes was observed using thermo gravimetric analysis. TG-DTA traces of all the prepared polymer electrolyte samples are shown in the Fig. 5.5(a- e) . In Fig. 5.5(a), the DTA curve shows a small endothermic peak at 70 °C, indicating the melting of the polymer film, and it exhibits a linear trend towards its decomposition temperature at 291 °C. This peak is concurrent with the TG curve.

Table 5.2. TG/DTA results of the prepared samples

Sample code	Decomposition range (°C)		% wt loss (± 2% at various temperatures (°C))		Endothermic peaks (°C)		Exothermic peaks (°C)	
	First	Second	100	200				
E1	60-70	230	8	16	70	-	-	291
E2	50-60	220	16	30	55	-	-	301
E3	50-60	236	12	13	55	-	-	295
E4	40-60	240	13	30	40	-	-	292
E5	55-70	250	9	25	55	-	-	369

The first and second decompositions of the film take place between 60-70 °C and 200-230 °C (Table 5.2), respectively, and the corresponding weight losses were 8% and 16% (Fig. 5.5(a)) at 100 °C and 200 °C, respectively.

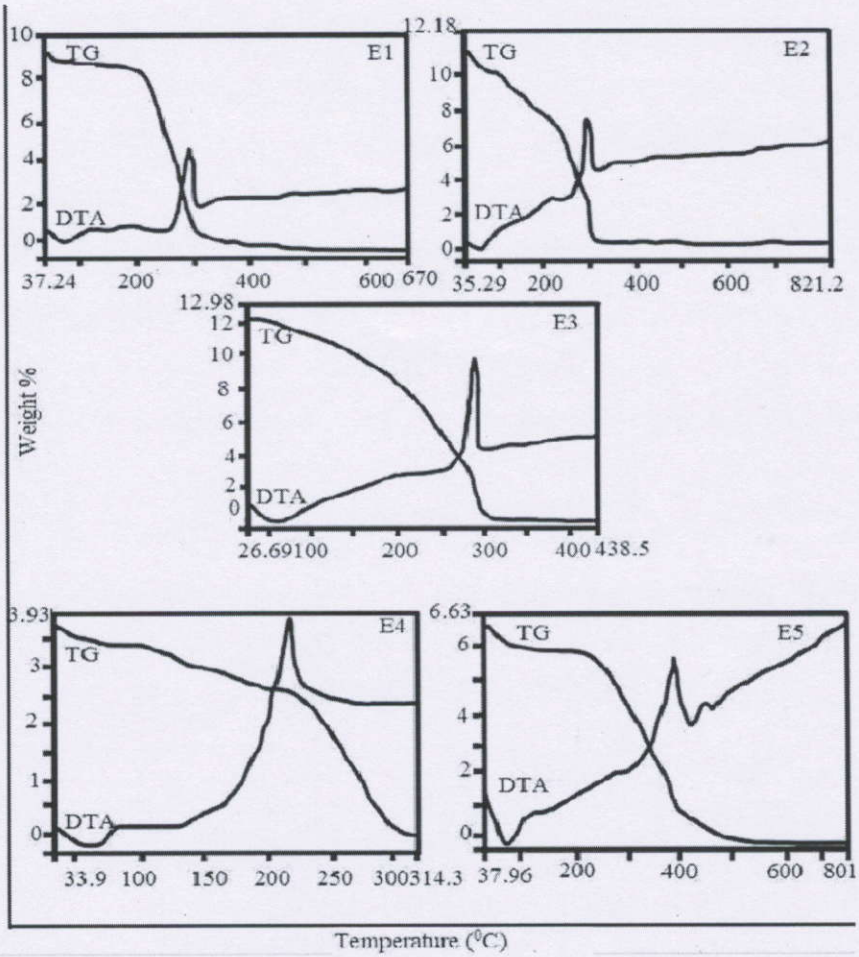

Figure 5.5. (a). TG/DTA curves of PVC(5)-PEMA(20)-$LiClO_4$(8)-PC(67)- TiO_2(0 wt %), (b). TG/DTA curves of PVC(5)-PEMA(20)-$LiClO_4$(8)- PC(67)- TiO_2(5 wt %), (c). TG/DTA curves of PVC(5)-PEMA(20)-$LiClO_4$(8)-PC(67)-TiO_2(10 wt %), (d). TG/DTA curves of PVC(5)-PEMA(20)-$LiClO_4$(8)-PC(67)-TiO_2(15 wt %), (e). TG/DTA curves of PVC(5)-PEMA(20)-$LiClO_4$(8)-PC(67)-TiO_2(20 wt %).

In the DTA curve (Fig. 5.5(b)), the melting of the polymer film is observed at 55-65 °C, which is indicated by a small endothermic peak. Followed by it, there is no other peak until 280 °C. This trend is accompanied by a rapid weight loss of the film E2. The thermal stability of the polymer film is found to be poor. The exothermic peak at 280°C corresponds to the decomposition of the polymer electrolyte. The first and second decompositions of the film take place in between 50-60 °C and 220-300 °C, respectively, and the corresponding weight losses were 16% and 30% at 100 °C and 200 °C, respectively.

In the DTA curve (Fig. 5.5(c)), the polymer film exhibits a linear trend beyond 55 °C at which an endothermic peak is observed which clearly indicates the melting of the polymer film. A large exothermic peak is observed in the temperature range 225-295 °C, indicating the final decomposition of the polymer film which is supported by the TG curve wherein the weight loss of the film is gradually decreasing. From the DTA and TG curves, it can be seen that, the thermal stability of the film is 236 °C. The first and second decompositions take place at 50 °C and 236 °C, respectively, and the corresponding weight losses were 12% and 13% at 100 °C and 200 °C, respectively.

In the DTA curve (film E4), the polymer film exhibits a linear trend beyond 40 °C at which an endothermic peak is observed. This peak indicates the presence of moisture at the samples. A sharp exothermic peak observed at 292 °C indicates the final decomposition of the polymer film, which is accompanied by the TG curve wherein the weight loss of the film is continuously decreasing. From the DTA and TG curves, it can be seen that, with the increase in the temperature, the film E4 loses its weight continuously, showing poor thermal stability. The first and second decompositions of the film take place in between 40-60 °C and 240 °C,respectively, and the corresponding weight losses were 13% and 30% at 100 °C and 200 °C, respectively. In the DTA curve (Fig. 5.5(e)), an endothermic peak is observed in the temperature range 55-70 °C, indicating the melting of the polymer film. A clear, larger exothermic peak is noticed in the temperature range 330-390 °C confirming the decomposition of the polymer film. The TG curve indicates no appreciable weight loss until 250 °C. The thermal stability of the polymer film is found to be at 250 °C in the TG curve. The first and second decompositions take place at 60 °C and 250 °C, respectively, and the corresponding weight losses were 9 and 25% at 100 °C and 200 °C, respectively. The conductivity value has been found to be maximum (7.179×10^{-3} S cm^{-1}) for the film E4 compared to other films. Hence, the film E4 is found to be superior among the other films on the basis of both thermal stability and conductivity.

Morphological Analysis

The scanning electron micrographs of 0, 15, and 20 wt% TiO_2 based PVC(5)-PEMA(20)-PC(67)-$LiClO_4$ (8) polymer electrolyte systems are shown in Fig. 5.6(a-c). No spherullitic structure due to crystalline phase are observed in Fig. 5.6(a,b). This confirms the amorphous nature of the developed electrolytes. As the content of TiO_2 increases, in Fig. 5.6(c) the film

surfaces become rough. Also, it is found that in Fig. 5.6 (c) the grain size increases, with a reduction in the number of grain aggregates that tend to restrict the ionicmovement. Consequently, the conductivity decreases.

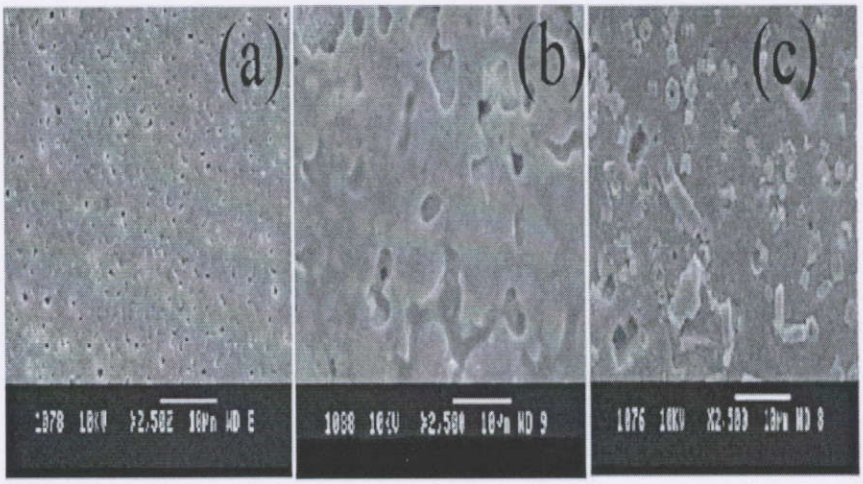

Figure 5.6. SEM images of (a) PVC(5)-PEMA(20)-$LiClO_4$(8)-PC(67)- TiO_2(0 wt %),
(b) PVC(5)-PEMA(20)-$LiClO_4$(8)-PC(67)-TiO_2(15 wt%),
(c) PVC(5)-PEMA(20)-$LiClO_4$(8)-PC(67)-TiO_2(20 wt%)

It is evident from the image of the surface of the film that the ceramic had not undergone any chemical reaction with the polymer. The 15wt% TiO_2 based complex shows that the ceramic particles present in the samples are more dispersed when compared with others.

Conclusion

The addition of nanofillers TiO_2 into the polymer blend matrix greatly enhances the amorphous region, which in turn improves the overall conductivity. The composite membrane containing 15 wt% TiO_2 nanofiller showed better ionic conductivity (7.179×10^{-3} S cm^{-1}), and the membrane is found to be thermally stable up to a temperature of 260 °C. The addition of plasticizer propylene carbonate (PC) enhances the amorphous phase as well as the charge carrier dissolution in the matrix. The XRD patterns revealed the dissolution of the lithium salt and it was found that excess filler content (above 15 wt%) builds a crystalline phase which causes a reduction in the ionic conductivity of the membranes. The complex formation has been confirmed from FTIR spectral studies. The salt-in-polymer electrolytes prepared from the PVC/PEMA show a strong enhancement of the ionic conductivity by the addition of TiO_2 nanoparticles. The ionic

conductivity of the resulting composite polymer electrolyte is better than the blend polymer electrolyte. The temperature dependent ionic conductivity plot of the composite films seems to obey the VTF relation. The porous natures have been identified using scanning electron microscopy. The optimized polymer electrolyte can be used as an electrolyte in the fabrication of Li batteries.

F. Preparation of polymer electrolyte films

Poly (ethyl methacrylate) PEMA (M_w=5,15,000) and $LiClO_4$ were procured from Sigma Aldrich chemicals limited, USA. The plasticizer propylene carbonate (PC) was obtained from Alfa Aesar and used as such. The solvent tetrahydrofuran (THF) was purchased from SRL, Mumbai and used without further purification. The ceramic fillers MWCNT (particle size ~ 30-50nm) and TiO_2 (particle size ~ <25nm) was purchased from Sigma Aldrich chemicals limited, USA. The polymer electrolytes consisting of PEMA with different fillers were prepared by solution casting technique.

Structural Analysis

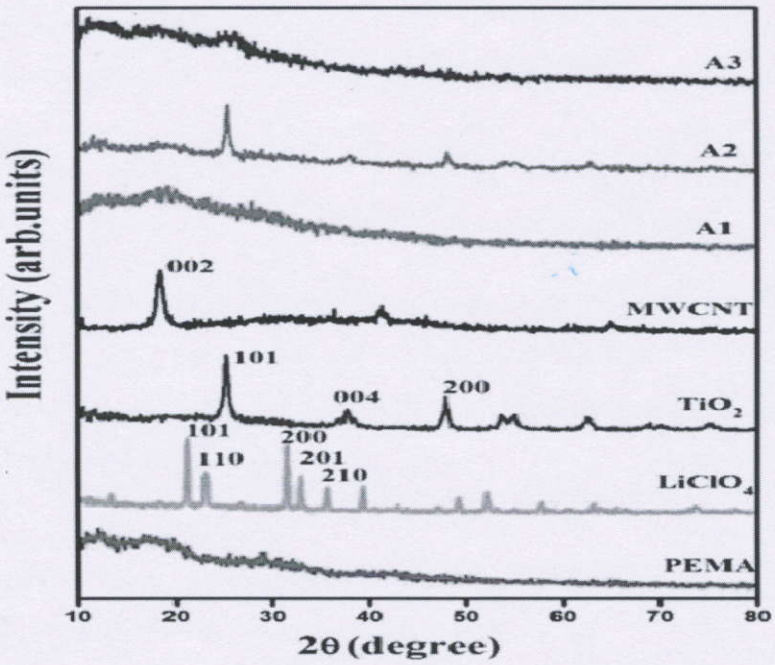

Figure 6.1. XRD patterns of pure PEMA, $LiClO_4$, TiO_2, MWCNT and blended polymer electrolytes.

Figure 6.1 shows the XRD patterns for pure PEMA, $LiClO_4$, TiO_2, MWCNT and prepared composite electrolytes. The pristine samples revealed a peak corresponding to the (002) crystalline plane of the MWCNT and the peaks at (101), (004) and (200) of TiO_2 respectively. The XRD pattern of pure $LiClO_4$ showed crystalline behaviour due to the appearance of peaks at (101), (110), (200), (201), (210) planes. But in the case of PEMA a diffraction hump is observed which reveals the amorphous nature. The XRD pattern of prepared composites containing MWCNT showed a remarkable reduction in the XRD peaks this is due to the destruction effect of the filler on the ordered arrangement of the polymer side chains. There is no obvious carbon diffraction peaks in PEMA-MWCNT composite due to its amorphous state. The shift and decrease in the relative intensity of the peaks suggest that complexation has occurred between the fillers and the polymer.

Conductivity Studies

The ionic conductivity of the films depends on the overall mobility of ion and polymer, which is determined by the free volume around the polymer chain. Table 6.1 shows the conductivity results of PEMA-$LiClO_4$-PC-Nanocomposite filler polymer electrolyte complexes.

TABLE 6.1. Temperature dependent ionic conductivity of the prepared samples.

Code	PEMA (19)-$LiClO_4$(8)-PC(67)-X (6) wt%	Conductivity values (σ) Scm^{-1} at different temperatures				
		303K	313K	323K	333K	343K
A1	X=0	$7.23X10^{-7}$	$8.22X10^{-7}$	$8.96X10^{-7}$	$9.05X10^{-7}$	$2.04X10^{-6}$
A2	X=6 (TiO_2)	$3.45X10^{-4}$	$4.53X10^{-4}$	$5.64X10^{-4}$	$5.98X10^{-4}$	$3.67X10^{-4}$
A3	X=6 (MWCNT)	$2.45X10^{-3}$	$2.87X10^{-3}$	$3.42X10^{-3}$	$3.86X10^{-3}$	$4.92X10^{-3}$

Ionic conductivity of the electrolyte films was found to be improved with the addition of MWCNT. The presence of filler particle enhances the ionic conductivity substantially and the degree of enhancement depends on the surface area of the filler. The steric hindrance effect of the ceramic filler contributed to the retention of the amorphous phase of polymer electrolyte and the ion transports mainly takes place by intra-chain and inter-chain hopping of ionic species in the amorphous region. As comparing the conductivity between MWCNT and TiO_2 with PEMA, the MWCNT composition encountered an increase in the conductivity. The inclusion of TiO_2 inert

oxide in PEMA results restrain growth of PEMA crystallites and exhibits conductivity but it does not exceeds the conductivity value of MWCNT composite electrolyte.

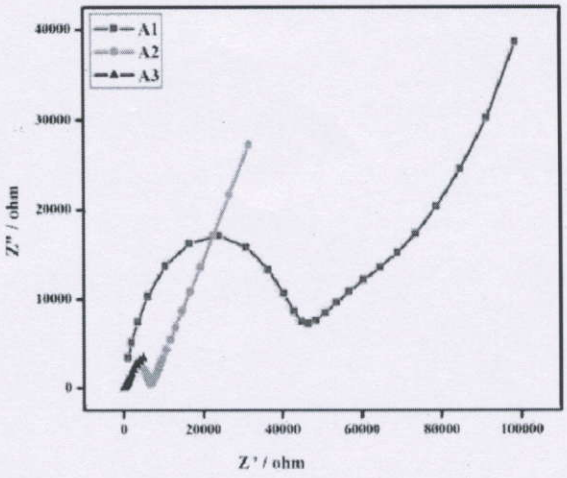

Figure 6.2. Room temperature complex impedance of the prepared samples.

Figure 6.2 shows the impedance spectra of PEMA-MWCNT composite, where the decreased semicircles in the medium frequency are related to the charge transfer process. The inclined lines in the lower frequency are attributed to the Warburg impedance, which is associated with lithium ion diffusion. It is obvious that the R_b drastically decrease and lithium ion diffusion coefficient increases when adding MWCNT. Therefore PEMA-MWCNT enhances the conductivity.

Dielectric Analysis

The dielectric behaviour of the polymer electrolyte system is described by using the dielectric function, ε^*. Figure 6.3 shows the plot of dielectric loss ε'' against the log ω for different temperatures. The higher dielectric loss is observed at lower frequencies and it decreases when the frequency increases. The large dielectric loss at lower frequency is due to free charges builds up at the interface between the electrolyte and the electrodes. At high frequencies, the periodic reversal of the electric field occurs so fast that there is no excess ion diffusion in the direction of the field. The polarization due to the charge accumulation decreases, leading to the decrease in the value of ε''.

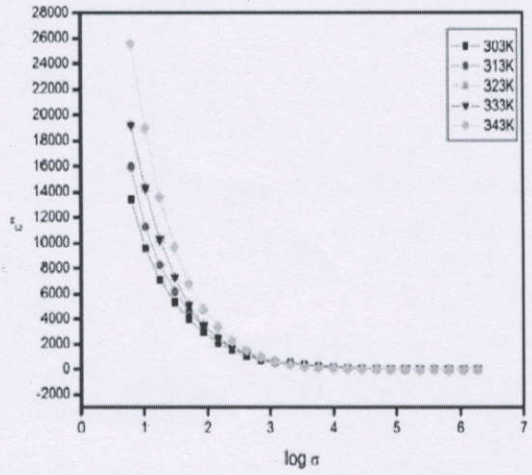

Figure 6.3. Variation of dielectric loss (ε″) as a function log ω for PEMA doped with MWCNT.

Dielectric relaxation spectra can provide information regarding the behaviour of the polymer electrolytes. The appearance of the dominant relaxation peak, whose maximum shifts gradually to higher frequencies with increasing temperature can be seen from the polymer electrolyte systems. As this peak was not present in the dielectric loss spectrum for pure PEMA, the peaks gets started appearing only after introducing the filler to the polymer. This is due to dielectric relaxation of ion pairs. As the ion pair relaxation frequency can be taken as a measure of the average ionic mobility in the electrolyte medium, provided that the polymer chain flexibility is rate determining for both ion pair rotation and ionic translation.

Conclusion

Polymer electrolyte based on PEMA (19wt%)-$LiClO_4$ (8wt%)-MWCNT (6wt%) has been developed and examined using XRD, impedance and dielectric analysis. The sample A3 containing 6wt% of MWCNT electrolyte showed ionic conductivity of $2.45 \times 10^{-3} Scm^{-1}$ at room temperature, which is the highest conductivity value for all investigated samples. These high values of a.c conductivity, dielectric loss at room temperature lead to make the sample as a promising material for lithium battery as an application in the solid state electrochemical devices.

G. Preparation of electrolyte and electrode

The PEO, PVdF-HFP, and $LiClO_4$ were dried in vacuum oven at 55 °C for 4 h to remove moisture. The ratios of PEO (6.25 wt%), PVdF-HFP (18.75 wt%), $LiClO_4$ (8 wt%), and PC (67 wt%) with different content of $BaTiO_3$ (0, 2, 4, 6, and 8 wt%) based electrolytes were prepared by solution casting technique with acetone as a solvent. Appropriate quantities of $LiClO_4$ were dissolved by adding in sequence to the solvent acetone. After incorporating the required amount of plasticizer PC, inorganic filler $BaTiO_3$ was suspended in the solution and stirred for about 48 h at room temperature before the electrolytes were cast on finely polished teflon supports or teflon-covered glass plates. The residual solvent was allowed to evaporate slowly at 40 °C in a vacuum oven for 48 h. The free standing films were obtained. The films are harvested and stored in highly evacuated desiccators to avoid the moisture absorptions. Flexible thin films with thickness of about 0.28 mm were obtained.

The composite cathode was prepared by mixing $LiFePO_4$ (active material), Super P Li carbon by Timcal (conductivity additive) and PVdF (binder) in the ratio 80:10:10 wt% using N-methyl pyrrolidone (NMP) as solvent. Then, the homogeneous viscous slurry was coated on the aluminum (Al) foil using doctor blade technique with the thickness of 25 μm. The resulting electrode was dried in a vacuum oven at 80 °C for overnight to remove the solvent; as-prepared dried electrode was pressed in between twin rollers to improve the adherence of the coating to the Al foil. Before cell assembly, the desired size of the active electrode (loading merely 8 mg) was dried in a vacuum oven at 80 °C for 12 h removing the residual solvent traces present in the electrodes. The activation of the prepared composite electrolytes and the fabrication of coin type cells were carried out in an argon-filled glove box with the oxygen and moisture level as <0.1 ppm.

Structural Analysis

Figure 7.1 a–d shows the XRD pattern of pure PEO, PVdF-HFP, $LiClO_4$, $BaTiO_3$, and the prepared composite polymer electrolytes. Figure 7.1d shows typical peak patterns for $BaTiO_3$ with a cubic structure as indexed in the standard data (JCPDS card no 31-174). The particle size of the inorganic filler $BaTiO_3$ was calculated using the Debye-Scherrer relation and found to be about ~100 nm.

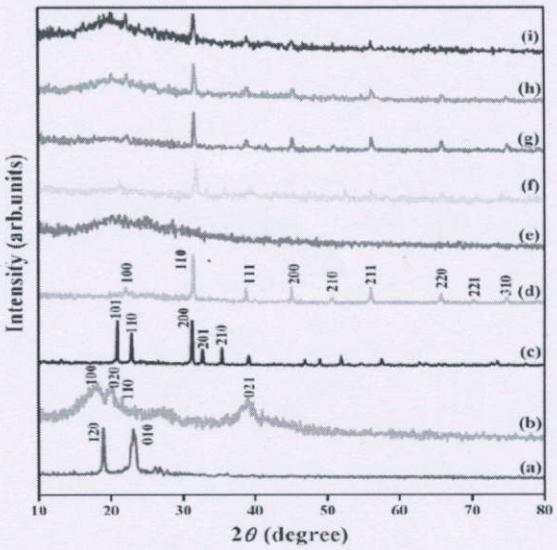

Fig. 7.1 XRD patterns of [a] pure PEO, [b] pure PVdF-HFP, [c] pure $LiClO_4$, [d] pure $BaTiO_3$, [e] PEO (6.25)-PVdF/HFP (18.75)-$LiClO_4$ (8)-PC (67)-$BaTiO_3$ (0).
[f] PEO (6.25)-PVdF/HFP (18.75)-$LiClO_4$ (8)-PC (67)-$BaTiO_3$ (2),
[g] PEO (6.25)-PVdF/HFP (18.75)-$LiClO_4$ (8)-PC (67)-$BaTiO_3$ (4),
[h] PEO (6.25)-PVdF/HFP (18.75)-$LiClO_4$ (8)-PC (67)-$BaTiO_3$ (6).
[i] PEO (6.25)-PVdF/HFP (18.75)-$LiClO_4$ (8)-PC (67)-$BaTiO_3$ (8)

In Fig. 7.1 a, two broad peaks are found at 2θ = 19.2° and 23.15° corresponding to the reflection of (120) and (010) plane, respectively, which confirms the semi-crystalline nature of PEO, which originates from the ordering of polyether side chains due to the strong intermolecular interaction between PEO chains through the hydrogen bonding. The peaks at 17.5°, 18.5°, 20.2°, and 39° correspond to lattice planes (100), (020), (110), and (021) semi-crystalline nature of PVdF-HFP as shown in Fig. 7.1b. Figure 7.1c shows high intense peaks at angles 2θ = 20.9°, 22.92°, 26.56°, 32.75°, and 35.4° corresponding to the lattice planes (101), (110), (200), (201), and (210) which reveal the crystalline nature of $LiClO_4$. Figure 7.1d reveals intense peaks at angles 22.10°, 31.45°, 38.8°, 45.12°, 50.76°, 56.07°, 65.75°, 70.21°, and 74.77° corresponding to the lattice planes (100), (110), (111), (200), (210), (211), (220), (221), and (310) of $BaTiO_3$.

In comparison with the pristine sample, the diffraction peaks of the composite polymer electrolyte containing PC and Li salt become considerably smaller and less prominent, reflecting the decrease in crystallinity. With the gradual addition of $BaTiO_3$ to the polymer matrix system,

the intensities of the characteristic peaks proportionally decreased, reaching the lowest value at 6 wt% concentration. Above this value, the intensity of the characteristic peaks increases with the increase of filler content (8 wt%) in the matrix.

It is now well recognized that the crystallization rate and degree of crystallinity can be influenced by crystallization in confined spaces. In these cases, the dimensions available for spherulitic growth are confined such that primary nuclei are not present for heterogeneous crystallization and homogeneous nucleation. The percentage of degree of crystallinity (χ) has been calculated and is found to be 49, 37, 33, 31, and 45 %, respectively, for the prepared samples 0, 2, 4, 6, and 8 wt% of $BaTiO_3$. This reduction in crystallinity upon the addition of inert filler is attributed to small particles of inert fillers which changes the chain re-organization and facilitates for higher ionic conduction.

The characteristic peaks corresponding to $BaTiO_3$ are impervious from its position in all the prepared electrolytes. After incorporating $BaTiO_3$ nanoparticle, these peaks hardly shift indicating that there are few changes of the crystal structure of the polymer matrix. However, the half widths of the crystal peaks decrease with the increase of the nanoparticle amount, indicating an increase in the amount of the amorphous phase. It is observed from the Fig. 7.1 e–i that the characteristic peaks that correspond to the lithium salts are mislaid in the complexes which confirmed the absolute dissolution of the salt in the polymer matrix.

Complexation Studies

Beside the porous structure of the polymer membrane, another effect on the electrochemical properties must be considered, which originates from the ion-dipolar interaction between Li^+-ions and the electron-withdrawing CF_2 groups of P(VdF-HFP). We thus measured the infrared spectra of the CPE to evaluate this ion-dipolar interaction. The presence of characteristics/functional group within the composite membrane is confirmed and depicted in Fig. 7.2.

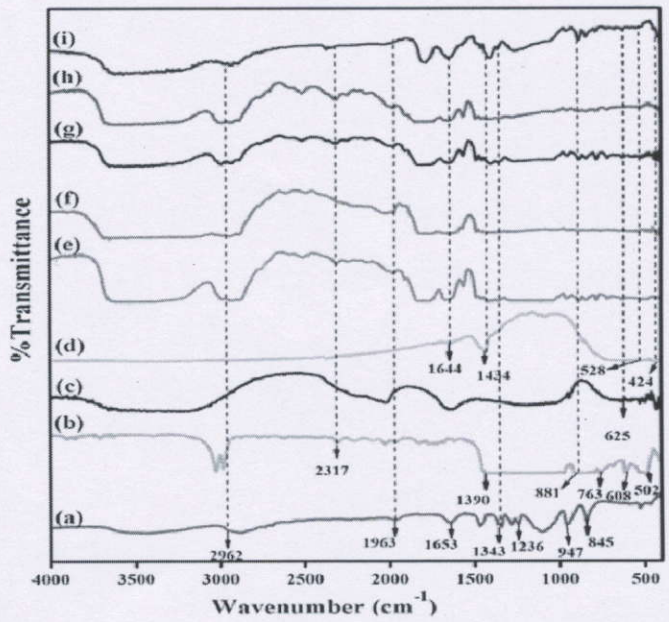

Fig. 7.2 FTIR spectra of [a] pure PEO, [b] pure PVdF-HFP, [c] pure $LiClO_4$, [d] pure $BaTiO_3$, [e] PEO (6.25)-PVdF/HFP (18.75)-$LiClO_4$ (8)-PC (67)-$BaTiO_3$ (0), [f] PEO (6.25)-PVdF/HFP (18.75)-$LiClO_4$ (8)-PC (67)-$BaTiO_3$ (2), [g] PEO (6.25)-PVdF/HFP (18.75)-$LiClO_4$ (8)-PC (67)-$BaTiO_3$ (4), [h] PEO (6.25)-PVdF/HFP (18.75)-$LiClO_4$ (8)-PC (67)-$BaTiO_3$ (6), [i] PEO (6.25)-PVdF/HFP (18.75)-$LiClO_4$ (8)-PC (67)-$BaTiO_3$ (8)

A large broad band between 2962 and 2823 cm^{-1} is ascribed to asymmetric C-H stretching of CH_2 of PEO that are shifted to (2964, 2958, 2962, 2968, 2966 cm^{-1}), (2823, 2826, 2831, 2822, 2827 cm^{-1}). Two narrow bands of lower intensity at 2735 and 2695 cm^{-1} are inherent bands of asymmetric (CH) stretching of CH_2 of PEO. The bands at 2238 cm^{-1} have C=O stretching combination and 2163 cm^{-1} assigned to asymmetric C–H stretching and C–H deformation combination of PEO that gets shifted to (2237, 2240, 2242, 2245, 2237 cm^{-1}), (2179, 2165, 2171, 2162, 2177 cm^{-1}), and (1967, 1972, 1972, 1972, 1972 cm^{-1}). The band at 1483 cm^{-1} represents the C–H bending of CH_2 in PEO that shifted to (1484, 1482, 1484, 1485, 1473 cm^{-1}). Very small intensity band occurs at 1799 cm^{-1} which corresponds to the ether oxygen group of PEO. The bands around 1359 and 1343 cm^{-1} are due to CH_2 wagging and CH_2 bending, respectively, which are characteristic of PEO. They are shifted to (1351, 1363, 1357, 1361, 1352 cm^{-1}) and (1340, 1346, 1342, 1340, 1338 cm^{-1}). The relatively small band at around 1236 cm^{-1} is assigned to CH_2 symmetric twisting of PEO, and these peaks are found at (1232, 1226, 1240, 1261, 1240 cm^{-1}).

The characteristic vibrational band at 1100 cm^{-1} was assigned to C–O–C (symmetric and asymmetric) stretching of PEO and was found at (1092, 1091, 1099, 1112 cm^{-1}). The two bands near 947 and 845 cm^{-1} are assigned to CH_2 rocking vibrations of methylene groups and are related to helical structure of PEO.

Apart from this, the mode responsible for the band at 845 cm^{-1} is primarily due to the CH_2 rocking motion with a little contribution from C–O stretching motion of PEO while the bands at 947 cm^{-1} originate primarily in the C–O stretching motion with some CH_2 rocking motion and these bands are shifted to (838, 846, 838, 840, 837 cm^{-1}) and (950, 953, 947, 955, 951 cm^{-1}). The vibrational peaks at 502 and 416 cm^{-1} are assigned to the bending and wagging vibrations of $–CF_2$, respectively, and get shifted to (499, 503, 509, 501, 507 cm^{-1}) and (414, 420, 422, 418, 416 cm^{-1}).

The crystalline phase of the PVdF-HFP polymer is identified by the vibrational bands at 985, 763, and 608 cm^{-1} and are shifted to (980, 983, 981, 979, 985 cm^{-1}), (779, 754, 773, 781, 779 cm^{-1}), and (601, 607, 605, 619, 603 cm^{-1}). The peaks at 1173 and 1390 cm^{-1} are assigned to the symmetrical stretching of $–CF_2$ and $–CH_2$ groups, respectively. The peak at 881 cm^{-1} is assigned to the vinylidene group of the polymer and shifted to (877, 883, 870, 881, 879 cm^{-1}). A strong absorption peak appears near 528 cm^{-1}; this peak characterizes the vibration of Ti–O octahedron which is shifted to (530, 516, 520, 534, 526 cm^{-1}). The characteristic peak at 528 cm^{-1} due to Ti–O stretching and the peak at 1434 cm^{-1} due to CO_3^{2-} of $BaTiO_3$ disappeared in composites whereas peak at 1644 cm^{-1} due to OH^- in $BaTiO_3$ spectra shifted to 1649 cm^{-1} in the spectra of the composites. FTIR bands at 1644 and 1434 cm^{-1} are due to OH^- and CO_3^{2-} vibrations, respectively, present in $BaTiO_3$. The band at 625 cm^{-1} corresponds to the ClO_4^- anion which is present in the complexes.

However, the width of this vibrational band is decreased with the increase of filler and $LiClO_4$ content. The effect of dopant on the modes of vibrations was observed in terms of decrease in the intensity, broadening of the bands with filler-salt content, and shifting of the bands to lower wave numbers. These behaviors indicate that there is a limit in the amount of lithium salt that can be dissolved in the polymer matrix. The above results suggest that the complexation takes place between the polymers, filler, and salt.

Conductivity Studies

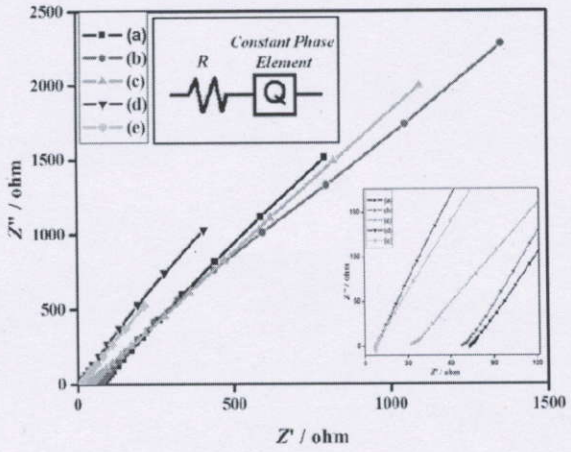

Fig. 7.3 Room temperature complex impedance plot of the prepared sample complexes.
[a] PEO (6.25)-PVdF/HFP (18.75)-$LiClO_4$ (8)-PC (67)-$BaTiO_3$ (0),
[b] PEO (6.25)-PVdF/HFP (18.75)-$LiClO_4$ (8)-PC (67)-$BaTiO_3$ (2),
[c] PEO (6.25)-PVdF/HFP (18.75)-$LiClO_4$ (8)-PC (67)-$BaTiO_3$ (4),
[d] PEO (6.25)-PVdF/HFP (18.75)-$LiClO_4$ (8)-PC (67)-$BaTiO_3$ (6),
[e] PEO (6.25)-PVdF/HFP (18.75)-$LiClO_4$ (8)-PC (67)-$BaTiO_3$ (8)

Figure 7.3 shows a typical impedance spectrum of PEO/PVdF-HFP-based membranes with $BaTiO_3$ at different concentrations. The ionic conductivity for temperatures above 30 °C was calculated using the resistivity obtained from a Nyquist plot as the intersection of impedance data with the real axis. The impedance responses are typical of the electrolytes where the bulk resistance is the major contribution to the total resistance and only a minor contribution from grain boundary resistance. The disappearance of the high frequency semicircular portion led to a conclusion that the current carriers are ions and this leads one to further conclude that the total conductivity is mainly the result of ion conduction. The straight lines that inclined toward the real-axis representing over the electrolyte electrode double layer capacitance behavior are obtained for all the samples. Experimental data can be fitted with the equivalent circuit, inserted in the corner (Fig.7.3), consists of ohmic resistance (R_1) representing the overall resistance of the membrane in series with the constant phase element. The constant phase element is a specific circuit element associated with current and potential distribution over an in-homogeneous electrode surface.

The conductivity of a solid-state electrolyte has many determinants, such as carrier concentration (Ci), mobility (μ_i), and so on. The interaction between the spontaneous polarization of the ferroelectric material and the ether oxygen of the adsorbed PEO should increase the dipole moment of the PEO chain, which would result in a conductivity increase in the interfacial region. It is well known that the more polar a solvent is, the greater the extent is to which lithium salts dissociate. In addition, the electrostatic interaction between the surface charge of ferroelectric particles and constituents of the salt should facilitate salt dissociation by stabilization of free ions, compared with neutral ion pairs, resulting in a shift of the dynamic equilibrium toward the free ions. The surface charge of $BaTiO_3$ particles may also produce a higher volume of the amorphous phase as a result of a higher nucleation rate during the solidification by acting as facile nucleation centers. Therefore, even for small amounts of added $BaTiO_3$, an increase in ionic conductivity of the (PEO)-PVdF-HFP-$LiClO_4$-$BaTiO_3$ composite electrolyte could be observed.

As commonly found in composite materials, the ionic conductivity is not a linear function of filler concentration. At low filler concentrations, the diffusion effect, which tends to depress conductivity, is effectively opposed by the specific interactions of the ceramic surfaces, which promotes fast ion transport. At higher filler concentrations, the dilution effect predominates; continuous non-conductive phase built up by large amount of filler as an electrically inert component would block up lithium-ion transport, resulting in an increase in the total resistance of the composite polymer electrolyte; and conductivity is reduced. The structural modifications on the filler surfaces may be due to the specific actions of the polar surface of the inorganic filler. The Lewis acid-base interaction centers react with the electrolytic species, thus lowering the ionic coupling, and promote the salt dissociation via a sort of ion filler complex formation. The effect of filler content on the ionic conductivity of the PEO/PVdF-HFP/$LiClO_4$-PC with $BaTiO_3$ at different contents 0, 2, 4, 6, and 8 wt% was examined. The filler content dependence of the ionic conductivity in the composite polymer electrolytes at temperatures of 303–373 K is shown in Fig.7.4. The ionic conductivity of the composite polymer electrolyte increased with an increase in filler content and reached a maximum value, then started decreasing with further addition of filler. The highest conductivity was obtained at the $BaTiO_3$ content of 6 wt%.

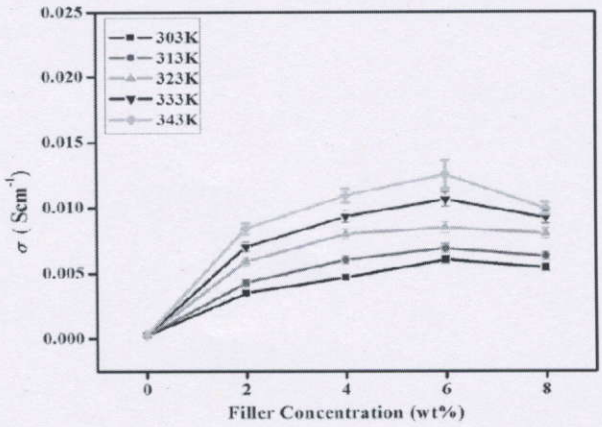

Fig. 7.4 Log σ vs filler concentrations of prepared complexes at different temperatures

The decrease in ionic conductivity at X = 8 wt% of $BaTiO_3$ can be discussed in view of molecular motion of PEO chain where it can strongly affect the movement of ions where Lewis acid-base interactions between the polar surface groups of $BaTiO_3$ and the electrolyte ions at high content of filler lead to the gauche arrangement of PEO back bone. The gauche conformation can decrease the segmental motion of PEO, and as a result, the conductivity decreases. Above the addition of 2 wt% of $BaTiO_3$, the high conducting regions are inter-connected to enhance the conductivity. The conductivity decreases after the addition of 6 wt% of $BaTiO_3$ that is generally related to the blocking effect of filler particles, which hinders the motion of mobile ions. It is well known that the electrical devices that work over a wide temperature range should have uniform conductivity with low activation energy.

Table 7.1 Ionic conductivity values, degree of crystallinity, porosity values, and activation energy for PEO (6.25 wt%)- PVdF-HFP (18.75 wt%)-$LiClO_4$ (8 wt%)-$BaTiO_3$ (X wt%) (where X = 0, 2, 4, 6, 8) polymer electrolyte systems

Film	$BaTiO_3$ ratio	Degree of crystallinity (%)	Porosity (10^{-6} m)	Activation Energy Ea	Ionic conductivity at various temperatures ($\times 10^{-4}$ Scm^{-1})				
					303 K	313 K	323 K	333 K	343 K
F1	0	49	1.01	0.40	2.395	2.569	2.714	2.846	2.913
F2	2	37	0.75	0.28	0.349	0.428	0.589	0.701	0.842
F3	4	33	2.52	0.22	0.467	0.602	0.798	0.093	0.010
F4	6	31	3.25	0.13	0.617	0.689	0.846	0.010	0.021
F5	8	45	0.81	0.36	0.542	0.628	0.803	0.922	0.919

The $BaTiO_3$ filler free sample that has activation energy (0.40 eV) higher than that for the $BaTiO_3$ filler samples (0.28, 0.22, 0.13, and 0.36 eV) is shown in Table 7.1. The decrease of activation energy can be attributed to an increase in the amorphous nature of the composite sample that will facilitate Li^+-ion motion in the polymer network.

Temperature dependence of ionic conductivity

The temperature dependence of the ionic conductivity in the composite polymer electrolytes at different composition of $BaTiO_3$ particles is shown in Fig.7.5.

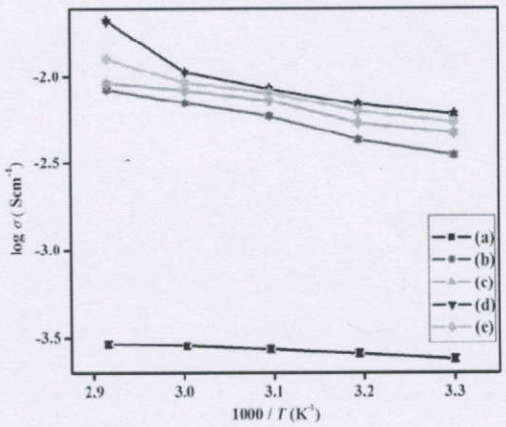

Fig. 7.5 Temperature-dependent ionic conductivity of the prepared sample complexes.

[a] PEO (6.25)-PVdF/HFP (18.75)-$LiClO_4$ (8)-PC (67)-$BaTiO_3$ (0),

[b] PEO (6.25)-PVdF/HFP (18.75)-$LiClO_4$ (8)-PC (67)-$BaTiO_3$ (2),

[c] PEO (6.25)-PVdF/HFP (18.75)-$LiClO_4$ (8)-PC (67)-$BaTiO_3$ (4),

[d] PEO (6.25)-PVdF/HFP (18.75)-$LiClO_4$ (8)-PC (67)-$BaTiO_3$ (6),

[e] PEO (6.25)-PVdF/HFP (18.75)-$LiClO_4$ (8)-PC (67)-$BaTiO_3$ (8)

The increase in σ_{ac} with temperature can be explained on the basis that rousing the temperature causes more structure relaxation and releasing more of Li^+-ions attached to oxygen of PEO to become more mobilized. This may be also due to the increase of drift mobility and hopping frequency of charge carriers. The frequency dependence of conductivity is also attributed to the change occurring in the mobility of charge carriers. As the temperature increases, the polymer tends to produce more free volume by expanding, resulting in the enhancement of the ionic and polymer segmental mobility. However, the ionic conductivity is not related linearly to the reciprocal temperature, suggesting that doping nano-$BaTiO_3$ does not change the conductive mechanism of the PEO-(PVdF-HFP)-$BaTiO_3$ and obeys the Vogel-Tamman-Fulcher (VTF)

equation reflecting the transport properties in a viscous matrix. This behavior is characteristic of the amorphous polymeric electrolytes that follow free-volume model, and the ionic transport mechanism is governed by free-volume theory. The role and the enhancement mechanism of nano-sized fillers at room temperature can be viewed from two points, namely, dielectric properties and the degree of crystallization. As the concentration is attained, on further addition of filler, a continuous non-conductive phase build up by large amount of fillers as an electrically inert component would block up lithium-ion transport, resulting in an increase in total resistance of the composite polymer electrolyte (CPE). It could be concluded that the addition of the $BaTiO_3$ content provided the most suitable environment for the ionic transportation and, thereby, achieved the highest conductivity. It was considered that the ion mobility of the CPE was enhanced due to the decreased crystallinity and beneficial features of the $BaTiO_3$ in comparison with those of the pristine electrolyte.

Dielectric Analysis

The dielectric behavior of the polymer electrolyte system is described by using the dielectric function, ε*. The complex permittivity of a system is defined by ε * = ε ' + iε" where ε′ is the dielectric constant (the real parts of complex permittivity) and ε″ is the dielectric loss (the imaginary part of complex permittivity). Using the impedance values, the dielectric loss can be calculated from the equation,

$$\varepsilon'' = \frac{Z'}{\omega C_o \left(Z''^2 + Z'^2\right)}$$

Here, Z′ and Z″ are the real and imaginary parts of the complex permittivity and $C_o = \varepsilon_o A/t$, ε_o is the permittivity of free space and $\omega = 2\pi f$, f is the frequency.

Figure 7.6 shows the plot of dielectric loss ε″ against the log ω for different temperatures. The higher dielectric loss is observed at lower frequencies, and it decreases when the frequency increases. The large dielectric loss at lower frequency is due to free charges built up at the interface between the electrolyte and the electrodes. At high frequencies, the periodic reversal of the electric field occurs so fast that there is no excess ion diffusion in the direction of the field. The polarization due to the charge accumulation decreases, leading to the decrease in the values of ε″.

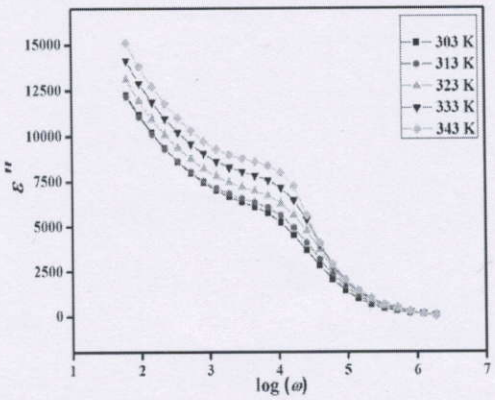

Fig. 7.6 Frequency dependence of dielectric permittivity for 6 wt% of doped $BaTiO_3$ at different temperatures

Dielectric relaxation spectra can provide important in-formation regarding the behavior of polymer electrolytes. The appearance of a dominant relaxation peak, whose maxi-mum shifts gradually to higher frequencies with increasing temperature, can be seen for the polymer electrolyte systems. As this peak was not present in the dielectric loss spectrum for pure PEO, PVdF-HFP started to appear only after introducing the filler and salt to the polymer. This is due to dielectric relaxations of ion pairs. As the ion pair relaxation frequency can be taken as a measure of the average ionic mobility in the electrolyte medium, the polymer chain flexibility is rate deter-mining for both ion pair rotation and ionic translation.

Thermal Analysis

TG-DTA traces of pure and composite PEO/PVdF-HFP with various concentrations of filler $BaTiO_3$ (0, 2, 4, 6, and 8 wt%) are depicted in Fig. 7.7a–e. It is observed from the curves that there is the initial weight loss of about 4–8 wt% in the temperature range of 25–70 °C for the prepared composite polymer electrolytes. This may be because of the moisture due to the loading of the sample and the weight loss is in agreement with the exothermic peak observed in the DTA curves of the samples around 40–55 °C. From the TG curve, it is also ob-served that the second decompositions occur around 120, 320, 155, 140, and 135 °C for the various concentrations of the $BaTiO_3$ system with the corresponding weight loss of about 14–22 wt%. It is found that the complete decomposition of the sample takes place between 327 and 387 °C with the corresponding weight loss of about 16–34 wt%.

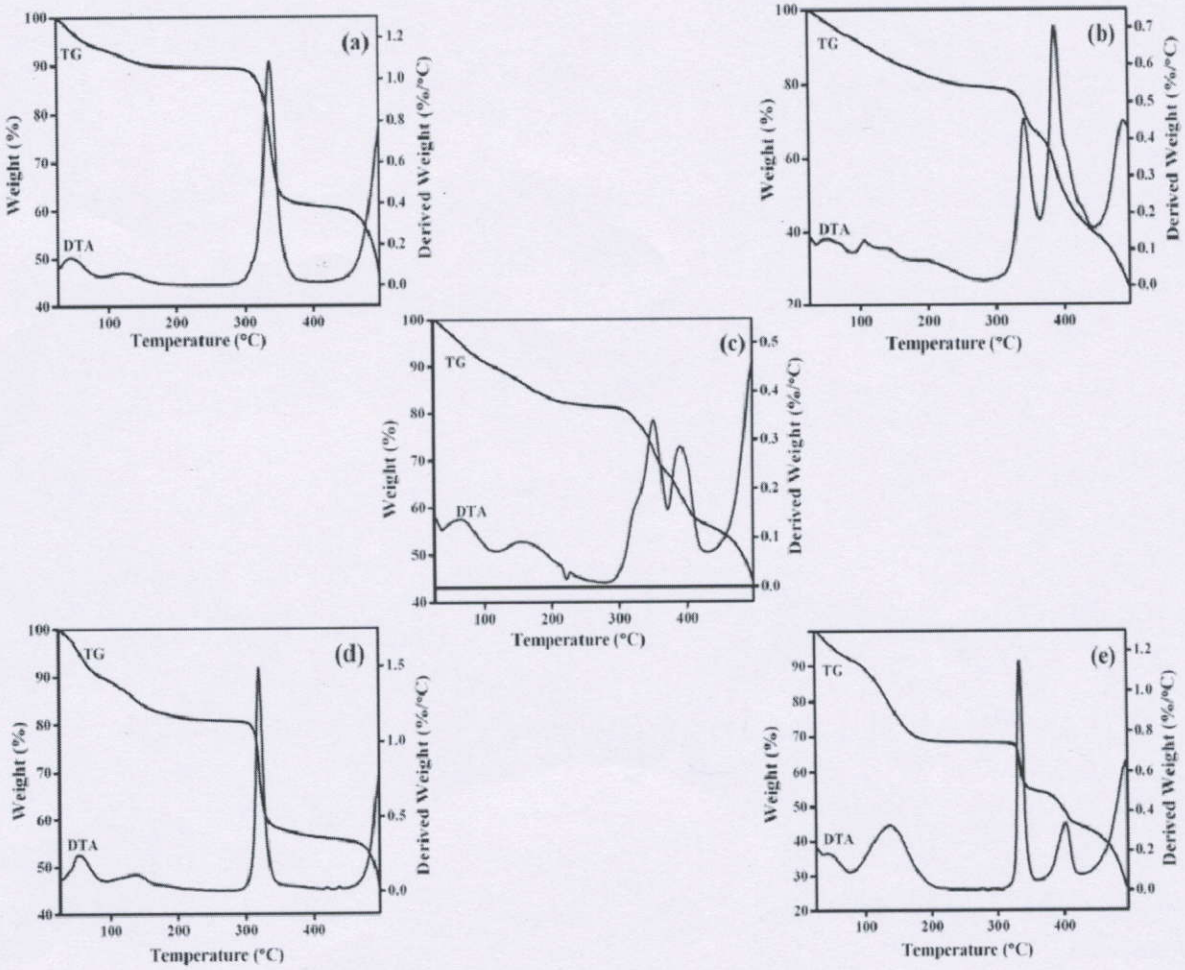

Fig. 7.7 TG-DTA analysis of the prepared complexes

[a] PEO (6.25)-PVdF/HFP (18.75)-$LiClO_4$ (8)-PC (67)-$BaTiO_3$ (0),

[b] PEO (6.25)-PVdF/HFP (18.75)-$LiClO_4$ (8)-PC (67)-$BaTiO_3$ (2),

[c] PEO (6.25)- PVdF/HFP (18.75)-$LiClO_4$ (8)-PC (67)-$BaTiO_3$ (4),

[d] PEO (6.25)-PVdF/HFP (18.75)-$LiClO_4$ (8)-PC (67)-$BaTiO_3$ (6),

[e] PEO (6.25)-PVdF/HFP (18.75)-$LiClO_4$ (8)-PC (67)-$BaTiO_3$ (8)

In DTA curve, the exothermic peaks occur in the range of 155–320 °C. This indicates the second decomposition of the polymer film, which is in good agreement with TG curve. Finally, it is concluded from the TG-DTA analysis that when the concentration of $BaTiO_3$ is increased, the thermal stability also increases up to 387 °C which is higher for the sample $BaTiO_3$ with 6 wt% compared to other samples. The sample with 6 wt% of $BaTiO_3$ exhibits thermal stability up to 327 °C, and the ionic conductivity is found to be maximum.

Trophological Studies

In the present study, two- and three-dimensional topographic images of the sample $BaTiO_3$ with 6 wt% having a maximum ionic conductivity are shown in Fig.7.8 a, b.

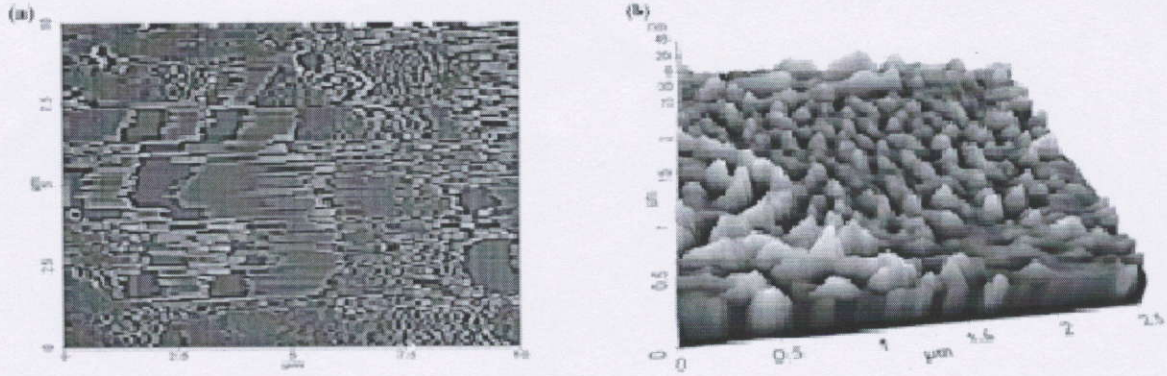

Fig. 7.8 Topography image of the maximum ionic conductivity sample.

[a] 2D image, [b] 3D image

The topographic images clearly show the presence of pores which are responsible for maximum ionic conductivity. The pores are helped to ensnare the large volume of the liquid in the pores accounting for the increased conductivity, and the presence of pores in the microstructure is mainly due to solvent removal and by solvent retention ability of the electrolyte system. The average roughness (R_{rms}) was calculated using the expression,

$$R_{rms} = \left(\frac{1}{N}\right)\sum_{i=1}^{N} |Z_m - Z_i|$$

where N is the number of deviations in height, (Z_i) from the profile mean value (Z_m). The composite polymer electro-lyte shows a clear mountain-valley pattern with more number of mountains and valleys. A well-defined mountain valley pattern with a roughness RMS value of 9.643 nm is observed for the surface of PEO-P(VdF-HFP)-$LiClO_4$-PC-$BaTiO_3$ sys-tem. The increase of roughness value for the polymer electrolyte over the polymer blend suggests that there is a good complexation between polymer and the filler used. It is observed that the root mean square roughness of the sample within the scanned area is found to be 12.224 nm. It could not see any small particles on the surface, indicating that the $BaTiO_3$ filler had been dispersed evenly into the host polymer. The good miscibility of the filler, lithium salt, and the host polymer was very

important prerequisite for good ionic conductivity. Increase of roughness value is observed for $BaTiO_3$ added system that led to the structural modification of the polymer system.

Morphological Analysis

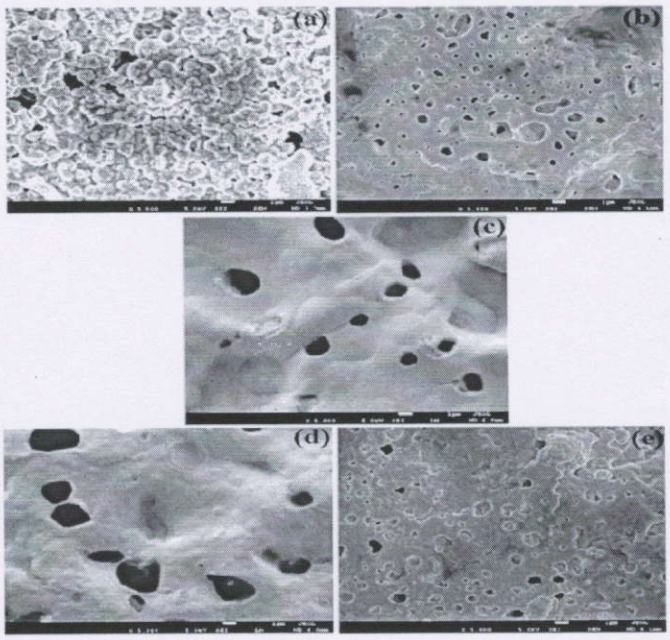

Fig. 7.9 Scanning electron microscope images of composite polymer electrolyte films containing [a] 0 wt%, [b] 2 wt%, [c] 4 wt%, [d] 6 wt%, [e] 8 wt% of $BaTiO_3$

In Fig. 7.9, compared with undoped membrane, the $BaTiO_3$-doped membranes possess smaller micro-pores and more interconnected pores, which suggest that the doped membranes can entrap more liquid electrolyte during the activated process and have higher ionic conductivity. These interconnecting structures may play a role in the increase of conductivity of this film because the network may present interconnecting pathways for conducting species to move through. The micro-graph for pure PEO/PVdF-HFP shows a rough surface which has several crystalline domains with large spherulites. After the addition of filler, the surface morphology of the polymer matrix is severely changed. It showed a dramatic improvement of surface morphology from rough to smooth. The smooth morphology was closely related to the reduction of PEO crystalline.

In Fig. 7.9b–e, it is notorious that the $BaTiO_3$ nanoparticles decorate the internal walls of the polymer pores, the fillers being located in the pore cavities instead of being incorporated within

the polymer matrix. Besides, the phases and the pores were made more prominent by increasing the $BaTiO_3$ content. Figure 7.9 shows that the pore size increases with increasing $BaTiO_3$ content which is to be ascribed to the filler effect on the bi-phase solvent-polymer phase diagram and therefore on the phase separation and solvent evaporation process. The defects in the electrolyte film disappeared suggesting that the film compactness had been removed. When filler content exceeds 6 wt%, the phase separation was observed due to immiscibility. Samples with higher amounts of filler have less free space in the pore cavities for the electrolyte liquid, resulting in lower electrolyte content. Further large pore sizes for a given degree of porosity leads to lower surface area for interaction between separator and electrolyte. No phase separation is observed in the image indicating that the fillers and the lithium salt do not contain any separate phases in the complex system and that the polymer blend is very compatible with the filler.

Galvanostatic characteristic evaluation of the polymer electrolyte in Li-ion half cell configurations

Evaluation in Li/$LiFePO_4$ cell

Charge-discharge characteristics of the composite polymer electrolyte membrane were evaluated using $LiFePO_4$ as cath-ode and lithium foil as anode. The electrolyte PEO (6.25 wt%)-P(VdF-HFP) (18.75 wt%)-$LiClO_4$ (8 wt%)-PC (6 wt%)-$BaTiO_3$ (6 wt%) is preferred to fabricate coin cell since it exhibits highest conductivity.

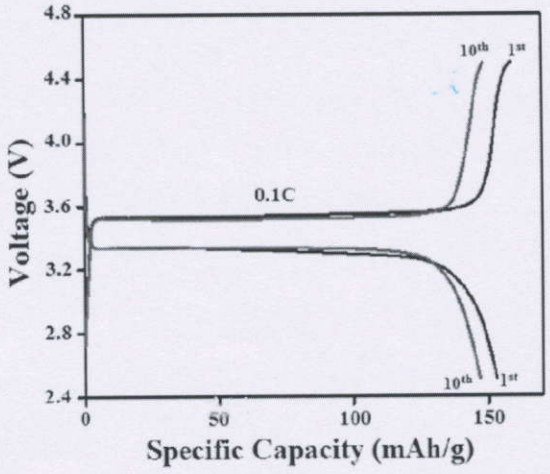

Fig. 7.10 Charge-discharge properties of $LiFePO_4$/CPE/Li cells with to the above said theoretical value of the $LiFePO_4$ electrode.

Figure 7.10 shows the charge/discharge curves of the cell assembled with as-prepared electrolyte membranes, which are obtained at a constant current of 0.1 C with operating voltage ranging from 4.5 to 2.5 V. For the cell with the PEO/PVdF-HFP composite membrane, it delivers that the potential during charge/ discharge voltage and two-stage plateau remains stable throughout cycling; the good performance of the CPEs can be attributed to the high ionic conductivity and stability of the membrane.

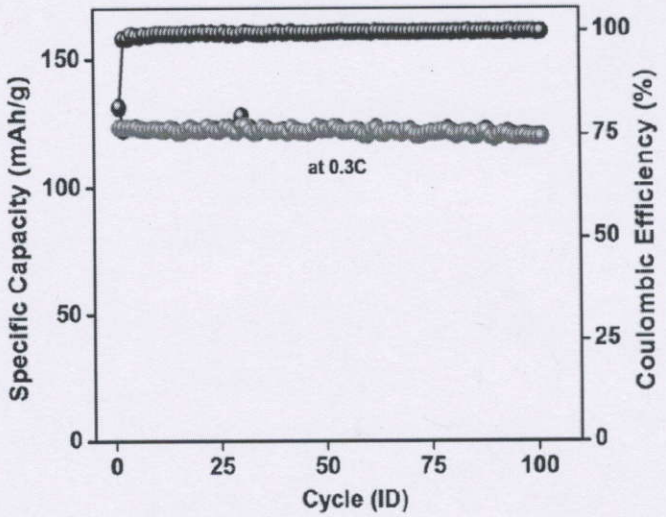

Fig. 7.11 Cycle performance of cells with coulombic efficiency at 0.3 C rate

It was noted that the cell with the PEO/PVdF-HFP-$BaTiO_3$ composite membrane delivered a discharge capacity of 153 mAh g^{-1} at 0 C. This value mainly depends on the electrode material used for the cell fabrication: in the present investigation, the electrode used has theoretical capacity of 170 mAh g^{-1}. The obtained value in the present study is close tested at different current rate. The cell performances obtained at different current rate are shown in Fig.7.11, and the results confirmed good cycle life capability of the cell and a relatively high specific capacity, 153 and 123 mAh g^{-1}, under low and medium C rates (0.1–0.3 C), respectively. It was observed that the significant capacity decreased to 106 mAh g^{-1} at the 0.5 C rate. However, the return to the lower current density (0.1 C) results in an increase in specific capacity (149 mAh g^{-1}). Thus, the voltage plateaus during charge-discharge process remain stable throughout cycling; the good performance of the CPEs can be attributed to the high ionic conductivity and stable mechanical property of the membrane.

The above results demonstrated the good electrochemical stability of the PEO/PVdF-HFP composite polymer electrolyte; this is another important factor that contributes to the cycle life.

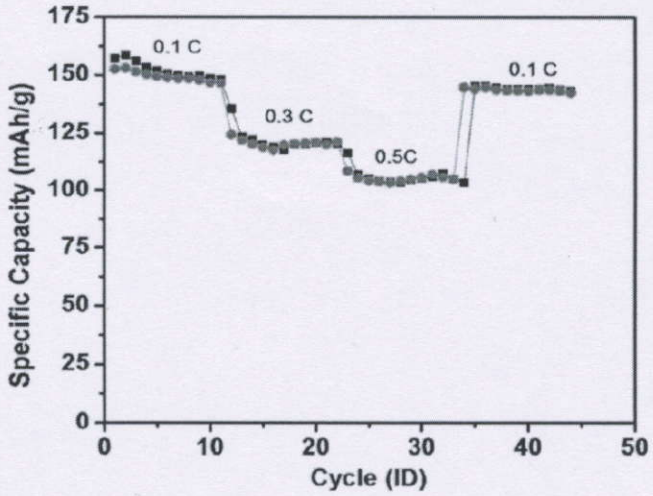

Fig. 7.12 Relationship between cycle performance and C rates of cells assembled with separators

Cycle life of the cell was evaluated at 0.3 C rates (Fig.7.12). The cell showed a charge and discharge capacity of 134 and 123 mAh g^{-1}, respectively, resulting in a coulombic efficiency of 93 %. In subsequent cycles, the coulombic efficiency in-creased to 99.6 % at the 100th cycles. The reversible capacity is not low, which is a good result and provides promising prospects for further research.

Our XRD and FTIR studies clearly show that at 6 wt% of doping $BaTiO_3$, there occurs reduction in crystallinity, de-crease in the intensity, and broadening of the bands. This amorphous nature produces greater ionic diffusivity in accordance with the high ionic conductivity. The enhancement in ionic conductivity is obtained only when adding high dielectric ceramic filler $BaTiO_3$ at 6 wt%, where the migrating ion species travel along the highly conducting pathway giving rise to the increase in ionic conductivity. Thermal stability exhibits maximum up to 327 °C for the sample with 6 wt% of $BaTiO_3$, and hence, the ionic conductivity is found to be maximum. AFM and SEM analysis reveals the morphology of the membrane having larger porosities with good miscibility of the filler, lithium salt, and the host polymer. It is very important prerequisite for good ionic conductivity

Conclusion

This present study demonstrated that the addition of ferroelectric $BaTiO_3$ enhanced the ionic conductivity of the composite polymer electrolyte films which is related to the high polarity of the filler. The ionic conductivity gradually increased to a maximum value of 6×10^{-3} Scm $^{-1}$ with adding 6 wt% $BaTiO_3$ filler. However, in the case of $BaTiO_3$ over 6 wt%, the ionic conductivity slightly decreased. These changes in the conductivity were mainly due to the increased crystallinity of PEO/PVdF-HFP resulting from an aggregation of particles at higher filler content. The ionic conductivity of the polymer electrolytes increases with increasing temperature and shows the VTF behavior. The activation energy decreases with in-creasing ionic conductivity at high temperatures and decreases upon the addition of salt, plasticizer, and filler. All of this may be related to a possible enhancement in the segmental flexibility of polymeric chains and the disordered structure of the electrolyte where the lithium-ion motion taking place in the amorphous phase is facilitated compared to the pure PEO sample. The inclusions of fillers create amorphous regions by the way of the interactions between the filler surfaces and the polymer chains, which result in the reduced crystallinity of the polymer that is characterized using XRD. The FTIR analysis confirms the shifts, broadening, and reduction in the intensity and the dissolution of the metal salt and filler in the polymer matrix. The TG-DTA study indicated that the thermal stability of the CPE was changed with the enhancement of the $BaTiO_3$ content. According to the results of TG-DTA thermograms, the conductivity enhancement is largely caused by the reduced glass transition temperature and PEO crystallite melting temperature due to the presence of salt, plasticizer, and filler. By increasing the $BaTiO_3$ content from 2 to 6 wt%, the film morphology was changed; it was confirmed by scanning electron microscope. However, when $BaTiO_3$ content exceeds 6 wt%, the CPE films showed the rather heterogeneous morphology. This was due to the immiscibility by the excessive addition of $BaTiO_3$. The polymer gel electrolyte performs with stable charge-discharge characteristics when evaluated as separator-cum-electrolyte in a lithium-ion cell. The results in the present study have shown that the presence of nano-sized ceramic fillers when hosted in PEO/P(VdF-HFP)-based composite membranes produces promising polymer electrolytes for lithium metal batteries.

vii. Other informations

a. Collaboration, if any (with Department, University, Industry etc,)

(i). Collaborated with the Department of Physical Chemistry, University of Madras, Chennai-600025 and published a paper.

"Structural and morphological studies on nanocomposite polymer blend electrolytes for Li battery applications", R. Sasikumar, **M.Ramesh Prabhu**, K.selvakumar, International Journal of Chemtech Research, 10(4) (2017) 390-396.

b. Ph. D Enrolled, if yes, details

(i) Mr. S. Edwinraj, who has been working in this project as Project fellow, enrolled his Ph.D. in Alagappa University, Karaikudi with Reg. No 800/2013-14 on 06/11/2013.

(ii) Mrs. P. Pradeepa enrolled his Ph.D. in Alagappa University, Karaikudi with Reg. No 785/2013-14 on 23/10/2013 and completed on 05.10.2016.

c. Details of the Publications resulting from the project work (please attach re-prints) letter of Acceptance of paper communicated.

Journals/Proceedings:

1. Investigations of effect of double plasticizers in PEMA-PVC based gel polymer blend electrolyte, S.Edwinraj, S.Benazir, **M. Ramesh Prabhu**; Research Teaching Learning letters, 14 (1) (2014) 1-5.
2. Preparation and characterisation of TiO_2 nano filler incorporated polymer composite for Li battery applications, P. Pradeepa, M. Priya, **M. Ramesh Prabhu**; Research Teaching Learning letters, 14 (1) (2014) 6 - 11.
3. Investigations on the addition of different plasticizers in (PVdF-HFP)/PEMA polymer blend electrolyte system, P. Pradeepa, **M. Ramesh Prabhu**, International Journal of ChemTech Research 7 (4) (2015) 2077 – 2084.

4. Preparation and characterization of MWCNT nanofiller incorporated polymer composite for lithium battery applications, P. Pradeepa, K. Selvakumar, S. Edwinraj, G. Sowmya, **M. Ramesh Prabhu***, AIP Conference Proceedings, 1665 (2015) 110011-1 – 110011-3

5. Effects of ceramic filler in Poly vinyl alcohol / Poly ethyl methacrylate based polymer blend electrolytes, P. Pradeepa, S. Edwin Raj, **M. Ramesh Prabhu*,** Chinese Chemical Letters, 26(9) (2015) 1191-1196.

6. Structural and electrochemical properties of PEMA with the influence of MWCNT / TiO_2 Filler, P. Pradeepa, S. Edwinraj, J. Kalaiselvimary, G. Sowmya, K. Selvakumar, **M. Ramesh Prabhu***, AIP Conference Proceedings,1731 (2016) 110037-1 – 110037-3.
7. Effect of different nanoparticles in PMMA/PVC based composite polymer electrolytes, **M. Ramesh Prabhu**, G. Sowmya, K. Selvakumar; Research Teaching Learning letters, 14 (1) (2014) 12-18.
8. Studies on electrical conductivity and thermal behaviour of PVAc/PVdF-HFP/Al_2O_3 polymer blend electrolytes, **M. Ramesh Prabhu** and D. Nagajothi, Research Teaching Learning letters, 14(1) (2014) 19-24.

9. Enhancement of the electrochemical properties with the effect of alkali metal systems on PEO/PVdF-HFP complex polymer electrolytes, Pradeepa Prabakaran, **Ramesh Prabhu Manimuthu***, Ionics, 22(6) (2016) 827-839.

10. Optimization of hybrid polymer electrolytes with the effect of lithium salt concentration in PEO/PVdF-HFP blends, P. Pradeepa, S. Edwinraj, G. Sowmya, J. Kalaiselvimary, **M. Ramesh Prabhu***, Materials Science and Engineering: B, 205 (2016) 6–17.

11. Electrochemical impedance and dielectric studies on PEO/PVA with NH_4Cl based proton conducting polymer electrolyte, S. Edwinraj, P. Pradeepa, K. Selvakumar, S. Mekala, **M. Ramesh Prabhu*,** Journal of Chemical and Pharmaceutical Sciences, 9(1) (2016) 172-174.

12. Composite polymer electrolyte based on PEO/PVdF-HFP with MWCNT for lithium battery applications, P. Pradeepa, S. Edwinraj, G. Sowmya, J. Kalaiselvimary, K. Selvakumar, **M. Ramesh Prabhu***, AIP Conference Proceedings, 1728 (2016) 020397-1 – 020397-4.

13. Dielectric behavior of different nanofillers incorporated in PVC-PMMA based polymer electrolyte membranes, G. Sowmya, P. Pradeepa, J. Kalaiselvimary, S. Edwinraj, **M. Ramesh Prabhu*,** AIP Conference Proceedings, 1728 (2016) 020413-1 – 020413-4.

14. Influence of Al_2O_3 on the structure and electrochemical properties of PVAc / PMMA based blend composite polymer electrolytes, P. Pradeepa, G. Sowmya, S. Edwinraj, G. Fareetha Begum, **M. Ramesh Prabhu***, Materials Today: Proceedings, 3 (2016) 2187-2196 ..
15. Effects of TiO_2 nanofiller incorporated polymer blend electrolytes for lithium battery applications, S. Ponmani, N. Anjali priya, P. Pradeepa, **M. Ramesh Prabhu***, International Journal for Research in Science Engineering and Technology-Proceedings, 3 (2016) 12-14.
16. Influence of barium titanate nanofiller on PEO/PVdF-HFP blend-based polymer electrolyte membrane for Li-battery applications, P.Pradeepa , G.Sowmya, **M. Ramesh Prabhu***, Journal of Solid State Electrochemistry (2016) DOI: 10.1007/s10008-016-3477-z
17. Plasticized polymer electrolyte membranes based on PEO/PVdF-HFP for use as an effective electrolyte in Lithium-ion batteries, P.Pradeepa , **M. Ramesh Prabhu***, G.Sowmya, S. Edwinraj, Chinese journal of polymer science, 35 (3) (2017) 407-421.

Conferences:

1. Investigation on PEG-2000/ PVC Based Polymer Blend Electrolytes Using Different lithium Salts, Second International Conference on Advanced Functional Materials (ICAFM 2014), CSIR-National Institute for Interdisciplinary Science & Technology, Thiruvananthapuram, February 19-21, 2014. **M. Ramesh Prabhu**, S. Edwinraj, V. Saranya.
2. Preparation and Characterisation of TiO_2 Nano filler incorporated Polymer Composite for Li Battery Applications, P. Pradeepa, M. Priya, **M. Ramesh Prabhu**; National Conference on Advanced Materials; Feb 24, 2014.
3. Investigations of Effect of Double Plasticizers in PEMA-PVC Based Gel Polymer Blend Electrolyte, S.Edwinraj, S.Benazir, **M. Ramesh Prabhu**; National Conference on Advanced Materials; Feb 24, 2014.

4. Preparation and Characterization of MWCNT Nanofiller Incorporated Polymer Composite for Lithium Battery Applications, P.Pradeepa, S.Edwin Raj, K.Selvakumar, G. Sowmya, **M.Ramesh Prabhu**, 59th DAE Solid State Physics Symposium (SSPS 2014), VIT University, Vellore, December 16-20, 2014.
5. Structural and Electrochemical Properties Of PEMA with the Influence of MWCNT / TiO_2 Filler, P. Pradeepa, S. Edwinraj, J. Kalaiselvimary, G. Sowmya, K. Selvakumar, **M. Ramesh Prabhu*,** 60th DAE Solid State Physics Symposium, Amity University, Noida, Uttar Pradesh, 21-25 December 2015.
6. Effects of nanofiller on electrochemical properties of polymer electrolytes for lithium batteries, S.Edwinraj, R.Kaladevi, **M.Ramesh Prabhu***, International conference on Frontier Areas in Chemical Technologies (FACTs-2016), Department of Industrial Chemistry, Bioelectronics & Biosensors, Nanoscience and Technology, Alagappa University, Karaikudi, 06 & 07 March 2016.
7. Studies on Electrical Conductivity and Thermal Behaviour of PVAC/PVDF-HFP/Al_2O_3 Polymer Blend Electrolytes, **M. Ramesh Prabhu** and D. Nagajothi; National Conference on Advanced Materials; Feb 24, August 2014.
8. Effect of Different Nanoparticles in PMMA/PVC-Based Composite Polymer Electrolytes, **M. Ramesh Prabhu**, G. Sowmya, K. Selvakumar; National Conference on Advanced Materials; Feb 24, August 2014.
9. Effect of double plasticizer in PVAc-PMMA based polymer blend electrolytes for Li-ion battery application, K. Selvakumar, **M. Ramesh Prabhu***, 3rd National Seminar on Technologically Important Crystalline and Amorphous Solids (TICAS-2014), Department of Physics, Kalasalingam University, Krishnankoil, 28th February & 01st March, 2014.
10. A Novel Solid Composite Polymer Electrolyte based on Poly(methylmethacrylate)/Poly (vinyl acetate) for Rechargeable Batteries, P. Pradeepa, G. Sowmya, R. Fareetha Begum, J. Kalaiselvimary, **M. Ramesh Prabhu***, National Conference on Advanced Materials (NCAM-2015), Department of Physics & Department of Electronics, St. Joseph's College, Tiruchirappalli, 06 February 2015.
11. Electrical and Thermal properties of double Plasticized polymer blend electrolytes based on PEO / P(VdF-HFP), P. Pradeepa, S. Eswari, **M. Ramesh Prabhu*,** National Seminar on

Frontier Areas in Chemical Technologies (FACTS-2015), Department of Industrial Chemistry, Alagappa University, Karaikudi, 06 & 07 March 2015.

12. Electrical and Thermal Properties of PVAc/PMMA Based Blend Composite Polymer Electrolytes for Lithium Battery Applications, P. Pradeepa, G. Fareetha Begum, **M. Ramesh Prabhu***, International Conference on Recent Advances in Nano Science and Technology (RAINSAT-2015), Sathyabama University, Chennai, 8-10 July 2015.
13. Composite Polymer Electrolyte Based on PEO/PVdF-HFP with MWCNT for Lithium Battery Applications, P. Pradeepa, S. Edwinraj, G. Sowmya, J. Kalaiselvimary, K. Selvakumar, **M. Ramesh Prabhu*,** International Conference on Condensed Matter & Applied Physics (ICC-2015), Government Engineering College, Bikaner, Rajasthan, 30&31 October 2015.
14. Dielectric behavior of different nanofillers incorporated in PVC/PMMA based polymer electrolyte membranes, G. Sowmya, P. Pradeepa, J. Kalaiselvimary, S. Edwinraj, **M. Ramesh Prabhu*,** International Conference on Condensed Matter & Applied Physics (ICC-2015), Government Engineering College, Bikaner, Rajasthan, 30&31 October 2015.
15. Electrochemical Properties of Organo-Montmorillonite Clay Nanocomposite Lithium Polymer Electrolytes Based on PEO/PVdF-HFP Blend, P. Pradeepa, R. Roshini, G. Sowmya, **M. Ramesh Prabhu*,** International conference on Frontier Areas in Chemical Technologies (FACTs-2016), Department of Industrial Chemistry, Bioelectronics & Biosensors, Nanoscience and Technology, Alagappa University, Karaikudi, 06 & 07 March 2016.
16. A Study on the effect of STA/APTEOS in the PVA Matrix based organic/inorganic composite Membranes, G. Sowmya, **M. Ramesh Prabhu***, International Seminar on Nanoscience and Technology (ISNST-2016), Department of Physics, Mother Teresa Women's University, Kodaikanal, 20 September 2016.
17. Effects of TiO_2 nano filler incorporated Polymer blend electrolytes for lithium Battery applications, S.Ponmani, N. Anjali priya, P. Pradeepa, **M. Ramesh Prabhu***, International Seminar on Nanoscience and Technology (ISNST-2016), Department of Physics, Mother Teresa Women's University, Kodaikanal, 20 September 2016.

Workshop:

1. UGC-DAE Consotium for Scientific Research University Campus, Khandwa Road, Indore(M.P.), Thematic Workshop on Physics of Phase Transitions, 24-25 October, 2013; S. Edwinraj.
2. School of Physics, Madurai Kamaraj University, One day Acqaintance Programme on Experimental Facilities at Inter University Accelerator Centre, Sponsored by IUAC-New Delhi, 15th November 2013; S. Edwinraj.
3. Indian Institute of Information Technology, Allahabad, 6th Science Conclave 2013, 08-14 December, 2013; S. Edwinraj.
4. School of Physics, Alagappa University, Karaikudi, International Workshop on Advanced Materials (IWAM-2014), 20&21 March,2014; S. Edwinraj.
5. Alagappa University, Karaikudi, Industry and Consultancy Cell & Centre for University Business Collaboration, 28 April, 2014; S. Edwinraj.

PRINCIPAL INVESTIGATOR REGISTRAR

(SIGNATURE WITH SEAL) (SIGNATURE WITH SEAL)